(12)

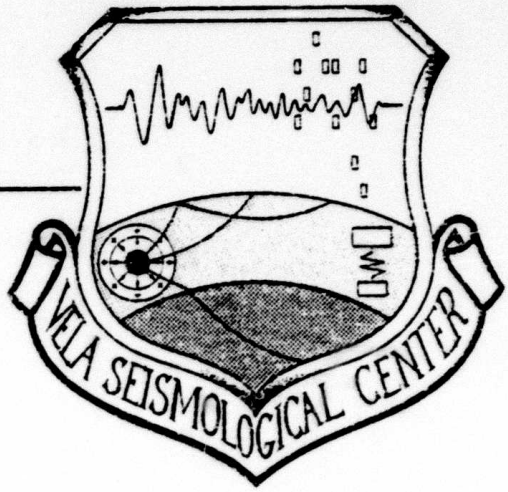


VSC-TR-83-1

# VERIFICATION OF THE EFFECTIVE STRESS AND AIR VOID POROSITY CONSTITUTIVE MODELS

J. T. Cherry
N. Rimer

TOPICAL REPORT

S-CUBED
P. O. Box 1620
La Jolla, California 92038

August 1982





Monitored by:

VELA Seismological Center
312 Montgomery Street
Alexandria, Virginia 22314

Unclassified

SECURITY CLASSIFICATION OF THIS PAGE (When Data Entered)

| REPORT DOCUMENTATION PAGE | | READ INSTRUCTIONS BEFORE COMPLETING FORM |
|---|---|---|
| 1. REPORT NUMBER<br>VSC-TR-83-1 | 2. GOVT ACCESSION NO.<br>AD-A124152 | 3. RECIPIENT'S CATALOG NUMBER |
| 4. TITLE (and Subtitle)<br>Verification of the Effective Stress and Air Void Porosity Constitutive Models | | 5. TYPE OF REPORT & PERIOD COVERED<br>Topical Report<br>6. PERFORMING ORG. REPORT NUMBER<br>SSS-R-82-5610 |
| 7. AUTHOR(s)<br>J. T. Cherry and N. Rimer | | 8. CONTRACT OR GRANT NUMBER(s)<br>F08606-79-C-0008 |
| 9. PERFORMING ORGANIZATION NAME AND ADDRESS<br>S-CUBED<br>P.O. Box 1620<br>La Jolla, California 92038 | | 10. PROGRAM ELEMENT, PROJECT, TASK AREA & WORK UNIT NUMBERS<br>ARPA Order No. 4436 |
| 11. CONTROLLING OFFICE NAME AND ADDRESS | | 12. REPORT DATE<br>August 1982<br>13. NUMBER OF PAGES<br>52 |
| 14. MONITORING AGENCY NAME & ADDRESS(if different from Controlling Office)<br>VELA Seismological Center<br>312 Montgomery Street<br>Alexandria, Virginia 22314 | | 15. SECURITY CLASS. (of this report)<br>Unclassified<br>15a. DECLASSIFICATION/DOWNGRADING SCHEDULE |

16. DISTRIBUTION STATEMENT (of this Report)

Approved for Public Release, Distribution Unlimited.

17. DISTRIBUTION STATEMENT (of the abstract entered in Block 20, if different from Report)

18. SUPPLEMENTARY NOTES

19. KEY WORDS (Continue on reverse side if necessary and identify by block number)

Constitutive models
Ground motion
Explosive source
Seismic coupling

20. ABSTRACT (Continue on reverse side if necessary and identify by block number)

In this report we present a severe test of the effective stress and air-void porosity constitutive models by using them to simulate experiments in which small scale explosions were detonated in grout spheres. High quality reproducible particle velocity data were obtained from these experiments. We show that an effective stress law coupled with the irreversible collapse of air-filled porosity provide a very simple, straightforward explanation of this data. These results have served to reenforce our confidence in the validity of these models and their importance in determining seismic coupling.

DD FORM 1 JAN 73 1473 EDITION OF 1 NOV 65 IS OBSOLETE

Unclassified

SECURITY CLASSIFICATION OF THIS PAGE (When Data Entered)

AFTAC Project Authorization No. VT/0712/B/PMP

ARPA Order No. 4436

Effective Date of Contract: November 17, 1978

Contract Expiration Date: November 15, 1981

Amount of Contract: $1,816,437

Contract No. F08606-79-C-0008

Principal Investigator and Phone No.

Dr. J. Theodore Cherry, (619) 453-0060

Project Scientist and Phone No.

Mr. Brian W. Barker, (202) 325-7581

This research was supported by the Advanced Research Projects Agency of the Department of Defense and was monitored by AFTAC/VSC, Patrick Air Force Base, Florida 32925, Under Contract No. F08606-79-C-0008.



W/O 11098

TABLE OF CONTENTS

LIST OF ILLUSTRATIONS

LIST OF ILLUSTRATIONS (Continued)

# I. INTRODUCTION

Of all the elements required for a numerical simulation of seismic coupling from a nuclear explosion, the most important and the most uncertain are the physical (constitutive) models of each nonlinear process induced in the medium by the propagating stress field, and the material properties required by the constitutive model which makes the simulation site specific. These two elements cannot be validated by numerical experiments. In fact, there is a trade-off between the two, with an incorrect constitutive model requiring incorrect material properties in order to produce results which agree with measured ground motion data.

Our approach to resolving this uncertainty has been to base the development and formulation of each constitutive model on the results of quasi-static laboratory tests on rock samples, and then to apply the model to the simulation of explosion induced ground motion. If the application appeared promising in terms of its ability to match ground motion data with the constitutive model using independently measured material properties, then the model was retained for use in future ground motion simulations.

This approach has shown that two specific constitutive models severely affect seismic coupling. They are, the irreversible collapse of air-filled porosity and the modification of material strength due to pore fluid pressure, i.e., effective stress. Therefore, the validation and testing of these models are issues of continuing importance and concern.

In this report, we present a rather severe test of these models by using them to simulate experiments in which small scale explosions were detonated in grout spheres. High quality, reproducible, particle velocity data were obtained from these experiments. We show that an effective stress law coupled with the irreversible collapse of air-filled porosity provide a very simple, straightforward explanation of this data. These results have served

to reenforce our confidence in both the validity of the effective stress and porosity constitutive models and the importance of these models for determining seismic coupling.

# II. CONSTITUTIVE MODELS FOR POROSITY AND EFFECTIVE STRESS

## 2.1 POROSITY

The first laboratory tests on the irreversible collapse of air-filled porosity in rock samples were reported by Stephens and Lilley (1970) in which they summarized their work on rocks of interest to the Plowshare Program. Based on this work, a constitutive model for porosity collapse was formulated (Cherry and Peterson, 1970), refined (Cherry, et al., 1973), and used to match ground motion data from explosive sources (Cherry and Peterson, 1970; Riney, et al., 1973).

These results were encouraging enough to suggest that we should use the model to determine the effect of air-filled porosity on teleseismic magnitudes. Cherry, Rimer, and Wray (1975) performed the parameter study and found that the introduction of porosity causes a severe reduction in magnitude with magnitude changing by 0.17 units when porosity changes from zero to one percent.

The porosity model developed by Cherry, et al. (1973) has essentially remained unchanged for our applications. In the model, the hydrodynamic component of the stress tensor, P, is dependent on air-filled porosity via a parameter, $\alpha$, given by

$$\alpha = \frac{V_r + V_\omega + V_p}{V_r + V_\omega} = \frac{v}{\hat{v}} \qquad (2.1)$$

where $V_r$, $V_\alpha$, and $V_p$ are the respective rock, water and air pore volumes, and v is the specific volume of the partially saturated mix.

The material properties required by the model are:

1. $\hat{P}(\hat{v})$, the pressure/volume relation for the rock with air-voids removed.
2. $P_c$, the pressure at which all air-voids are removed.
3. $P_e$, the pressure above which irreversible removal of air-voids begins.

4. $\phi_0$, the initial air-void volume fraction, where $\phi_0$ and $\alpha_0$ are related by

$$\alpha_0 = \frac{1}{1 - \phi_0} \quad . \tag{2.2}$$

5. $k_0$, the zero pressure bulk modulus of the porous mixture.

Given the above material properties, then

$$P = \frac{1}{\alpha} \hat{P}(v/\alpha) \tag{2.3}$$

where

$$\alpha_0 \geq \alpha \geq 1 \tag{2.4}$$

and the material properties ($P_c$, $P_e$, $\phi_0$, and $k_0$) determine the variation of $\alpha$ with $v$ under the constraints for pore collapse assumed by Cherry, et al. (1973).

As noted earlier, this model has been used successfully in a variety of ground motion simulations since its development. In this report we present additional evidence that the model adequately matches observed ground motion in rock materials whose air-void porosities range between 1.5 percent and 13.4 percent.

## 2.2 EFFECTIVE STRESS

The development of constitutive models for an adequate treatment of material strength has been an issue of debate and uncertainty among the ground shock calculation community for over ten years. The major issue may be stated as follows: "Given laboratory measurements of the static strength of rock, what are the appropriate values to be used in simulating the response of rock to an underground nuclear explosion?" The uncertainties associated with answers to this question arise because laboratory measurements

of strength vary greatly depending whether the sample is wet or dry, fractured or intact, and on the strain rate at which the test is conducted.

However, there is a minimum strength for a rock mass; i.e., the limit when the rock is completely broken into blocks. In this case Byerlee (1979) has shown that the strength is determined by the frictional strength, which is

$$\tau = 0.85\,\sigma_n \tag{2.5}$$

where $\tau$ is the shear stress and $\sigma_n$ the normal stress applied to the frictional surface. Equation (2.5) is applicable at low normal stresses ($0.2\ \text{Kb} < \sigma_n < 2.0\ \text{Kb}$). At higher normal stress, the applicable law is

$$\tau = 0.5 + 0.6\,\sigma_n \tag{2.6}$$

expressed in kilobars. Equations (2.5) and (2.6) have been shown to be independent of lithology, temperature and scale, and to exhibit a weak rate dependence in which the frictional strength decreases a few percent per decade of increase in sliding velocity (Scholz and Engelder, 1976; Dieterich, 1978).

When the rock contains a fluid within its pore structure at an internal pressure, $p_f$, it has been shown (Garg and Nur, 1973) that the strength of the rock does not depend only on the externally applied stress, but on an effective stress $(\sigma_n - p_f)$. For example, when fluid is present in the rock, Equations (2.5) and (2.6) should be modifed to be

$$\tau = 0.85\,(\sigma_n - p_f) \tag{2.7}$$

and

$$\tau = 0.5 + 0.6\,(\sigma_n - p_f) \tag{2.8}$$

and the strength is said to obey a "law of effective stress."

Even the synthesis of a large amount of data as represented by Equations (2.7) and (2.8) involves a large variation in strength, $\tau$, depending on the variation of pore pressure, $p_f$, with the stress state, $\sigma$. One might assume that the issue could be resolved by testing rock samples obtained from core taken at the site of the event. In general, this has proven to be an unsatisfactory procedure because the rock sample is not representative of the average water content or fracture density of the site, and because the laboratory induced pore pressure does not correspond to that generated in situ during the passage of the shock wave.

Therefore, due to the wide range of strength values available from laboratory tests, the only way to decide what is important is to try to match ground motion data from explosive sources, compare the strength required to match the data with that from laboratory tests, and then attempt to draw general conclusions concerning the types of laboratory tests most appropriate for the nuclear test rock environment. That is the approach we have taken.

The conclusions we have reached regarding the strength required to simulate explosive induced ground motion in low porosity brittle rocks (crystalline igneous rocks, crystalline metamorphic rocks, and well-consolidated sedimentary rocks) and high porosity brittle rocks (poorly consolidated sedimentary rocks and vesicular igneous rocks) are as follows:

1. The strength assumes a "high" value during the initial portion of the stress pulse and then relaxes to a "low" value.

2. The "high" value appears to be that obtained from laboratory measurements on dry rock samples. However, there is some evidence which indicates that for high strain rates ($10^4$ - $10^6$/sec), a strain rate effect should be added to the static dry strength measurements.

3. The low value appears to be that obtained by assuming that an effective stress law is operative and that the pore fluid pressure, $p_f$, is equal to the pressure of the externally applied stress, P.

Apparently the first to recognize the importance of effective stress for matching explosively induced ground motion data were Cherry and Peterson (1970). They assumed that the wet strength was the "equilibrium" strength, added a strain rate dependence to the dry strength, used a Maxwell solid formulation to relax between the dry and wet strengths, and succeeded in matching the stress history data obtained from small scale experiments in blocks of grout. Figure 2.1 shows the differences in measured strength characteristic between dry and wet grout. Figure 2.2 shows the comparison between the measured and calculated stress history, 6.5 centimeters from the charge, in grout with 10 percent air-void porosity, where the calculation was performed assuming relaxation between the strain rate dependent dry strength and the wet strength.

This model was revised by Cherry and Rimer (Bache, et al. 1975) where they used an effective stress law and coupled the Maxwell solid stress relaxation from the dry to the saturated strength with the removal of all air-void porosity from the rock matrix.

The last modification to the strength constitutive model has involved replacing the Maxwell solid relaxation with a direct calculation of the change in pore fluid pressure as a function of the parameter $\alpha$. In the model, we assume that the effective pressure, $P-p_f$, varies as follows:

$$P - p_f = P \qquad \alpha > \alpha_e \qquad (2.9a)$$

$$P - p_f = \left(\frac{1 - \alpha}{1 - \alpha_e}\right) P \qquad \alpha_e \geq \alpha \geq 1 \qquad (2.9b)$$

$$P - p_f = 0 \qquad \alpha = 1 \qquad (2.9c)$$

where $\alpha$ and P are defined by Equations (2.1) and (2.3) respectively, and

$\alpha_e$ is the value of $\alpha$ at $P_e$.

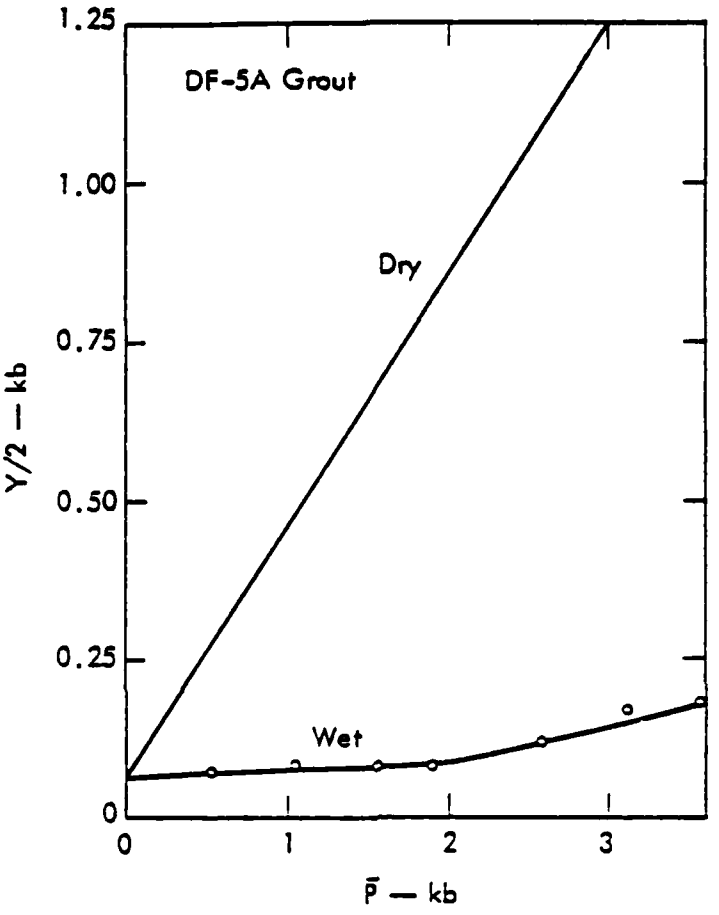


Figure 2.1. Strength of DF-5A grout (Cherry and Peterson, 1970). In this figure and in the remainder of this report, Y corresponds to the difference between the maximum and minimum principal stresses at failure under triaxial stress conditions and $\bar{P}$ is half the sum of these stresses. For a definition of these parameters in terms of stress invariants, see Cherry and Peterson (1970).

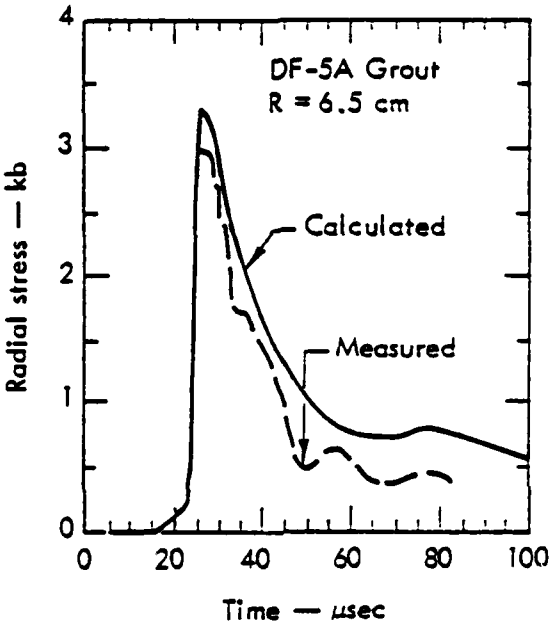


Figure 2.2. Stress history in DF-5A grout 6.5 cm from high explosive detonation (Cherry and Peterson, 1970).

The modifications given by Equation (2.9) were introduced into the model both to improve the physics in the model so that effective stress could be used directly in the calculation of strength, and to remove the strain rate dependence of the Maxwell solid which obviates the cube root scaling of ground motion measurements with explosion yield. The material strength is given by

$$Y = Y(\bar{P} - p_f) \tag{2.10}$$

with the strength function determined from laboratory tests on dry ($p_f$=0) rock samples. Equation (2.10) is intended to be a generalization of the effective stress law given by Equations (2.7) and (2.8). The reduction in strength due to $p_f$ is introduced into the calculation of strength via the effective stress constitutive model given by Equations (2.9) and (2.10).

It is worth emphasizing that the effective stress constitutive model makes simple and straightforward requirements on material properties data, with the critical material properties being the dry strength, $Y(\bar{P})$, and the pressure, $P_c$, at which all air voids are removed. Even if site specific measurments of these mterial properties are not available, enough laboratory tests have been conducted on a variety of rock types so that in most cases reasonable estimates of these properties can be made, e.g., Stephens and Lilley (1970), Heard (1970), Byerlee (1979).

Our first application of this model involved a simulation of ground motion data recorded from the 60 KT PILEDRIVER event. The material properties used for the simulation were obtained from Heard (1970) for the strength of dry, fractured granite, and from Brace (1965) for the pressure ($P_c$ = 1 Kb) at which all void space (fracture porosity) is closed. In addition, we assumed that the site contained 0.1 percent air void porosity.

Figure 2.3 and 2.4 compare the calculations with radial ground motion data recorded at a horizontal range of 204 meters. Figures 2.5 and 2.6 show a comparison between the data at 204 meters and a

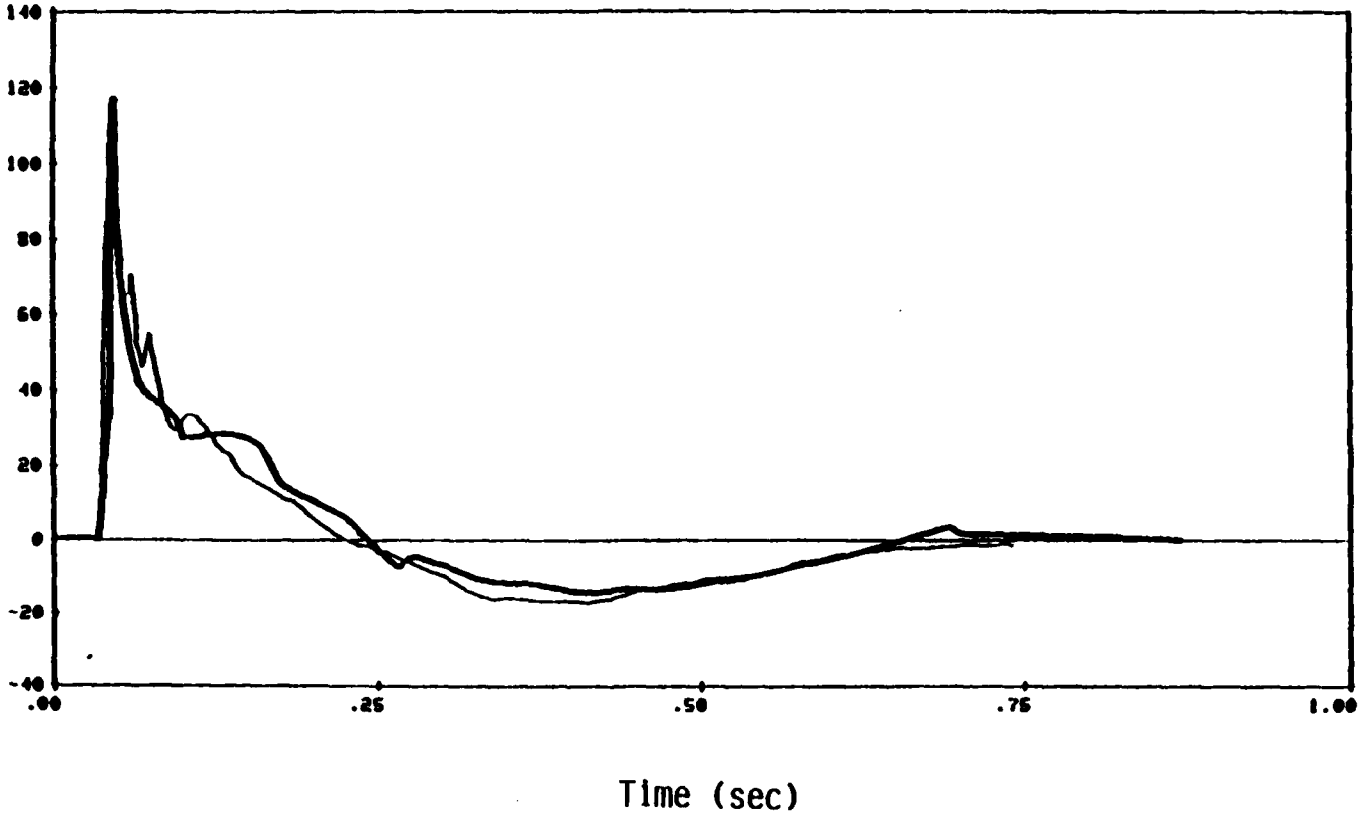


Figure 2.3. Comparison between PILEDRIVER particle velocity data (light curve) and the effective stress law calculation (heavy curve) 204 meters from the source.

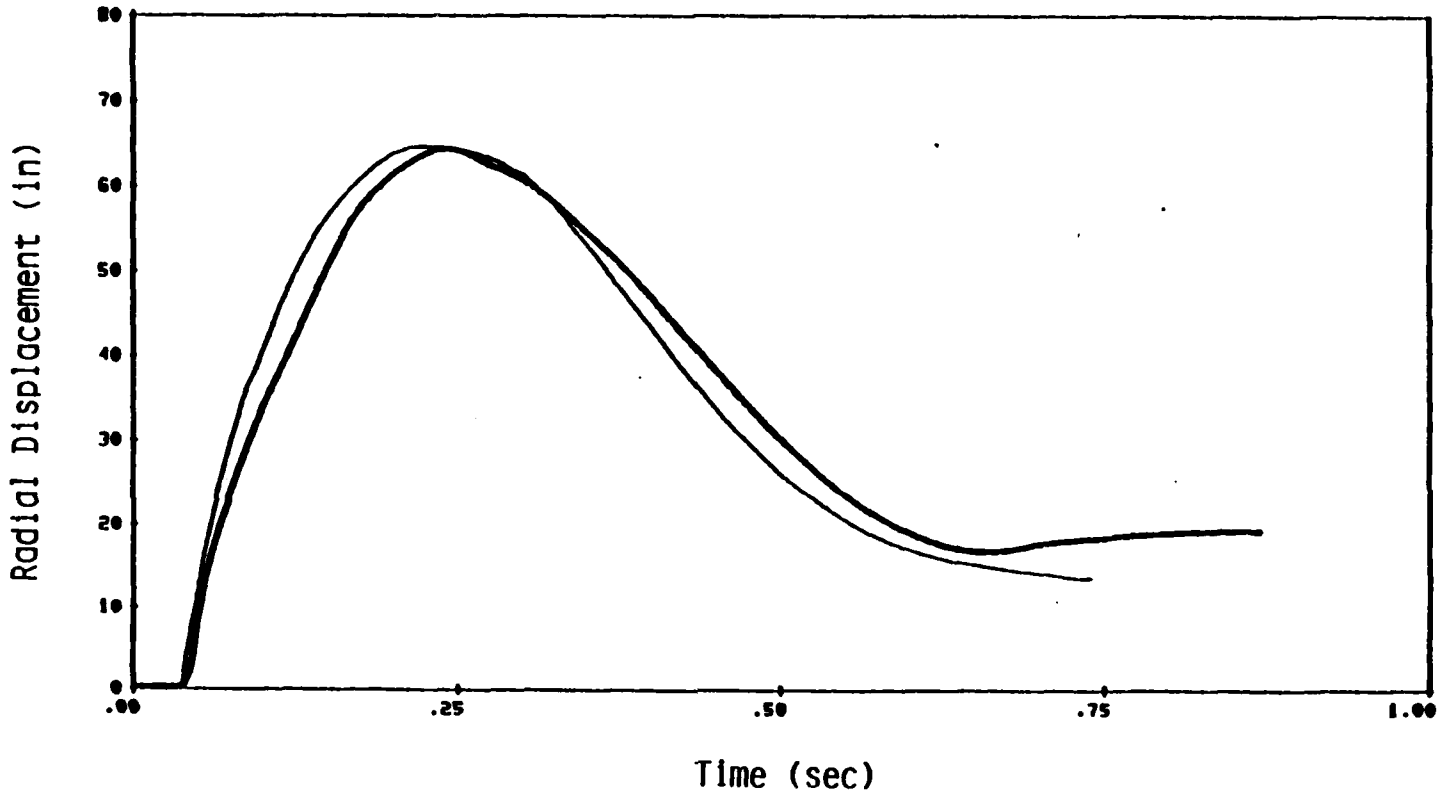


Figure 2.4. Comparison between PILEDRIVER displacement data (light curve) and the effective stress law calculation (heavy curve) 204 meters from the source.

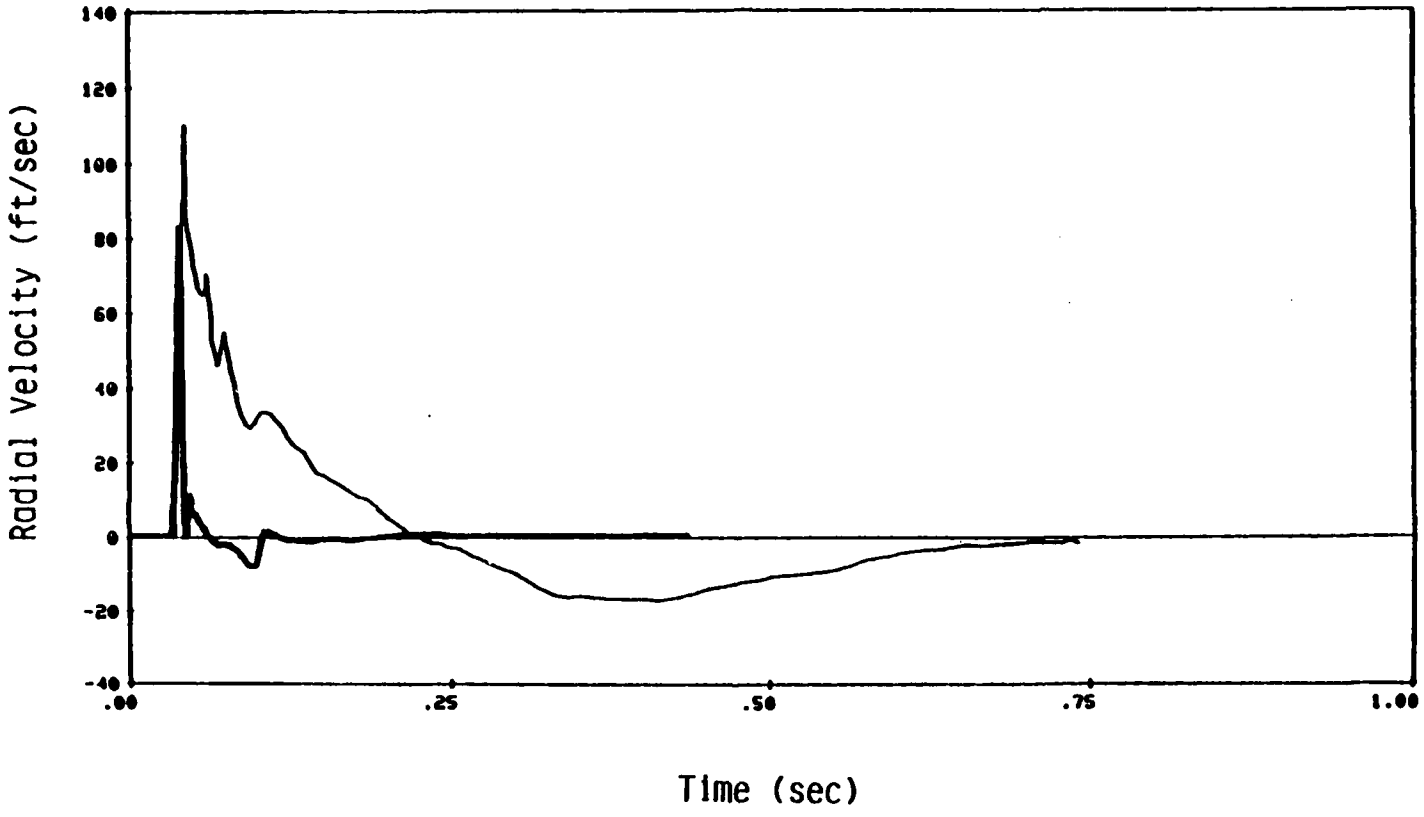


Figure 2.5. Comparison between PILEDRIVER particle velocity data (light curve) and the noneffective stress law calculation 204 meters from the source.

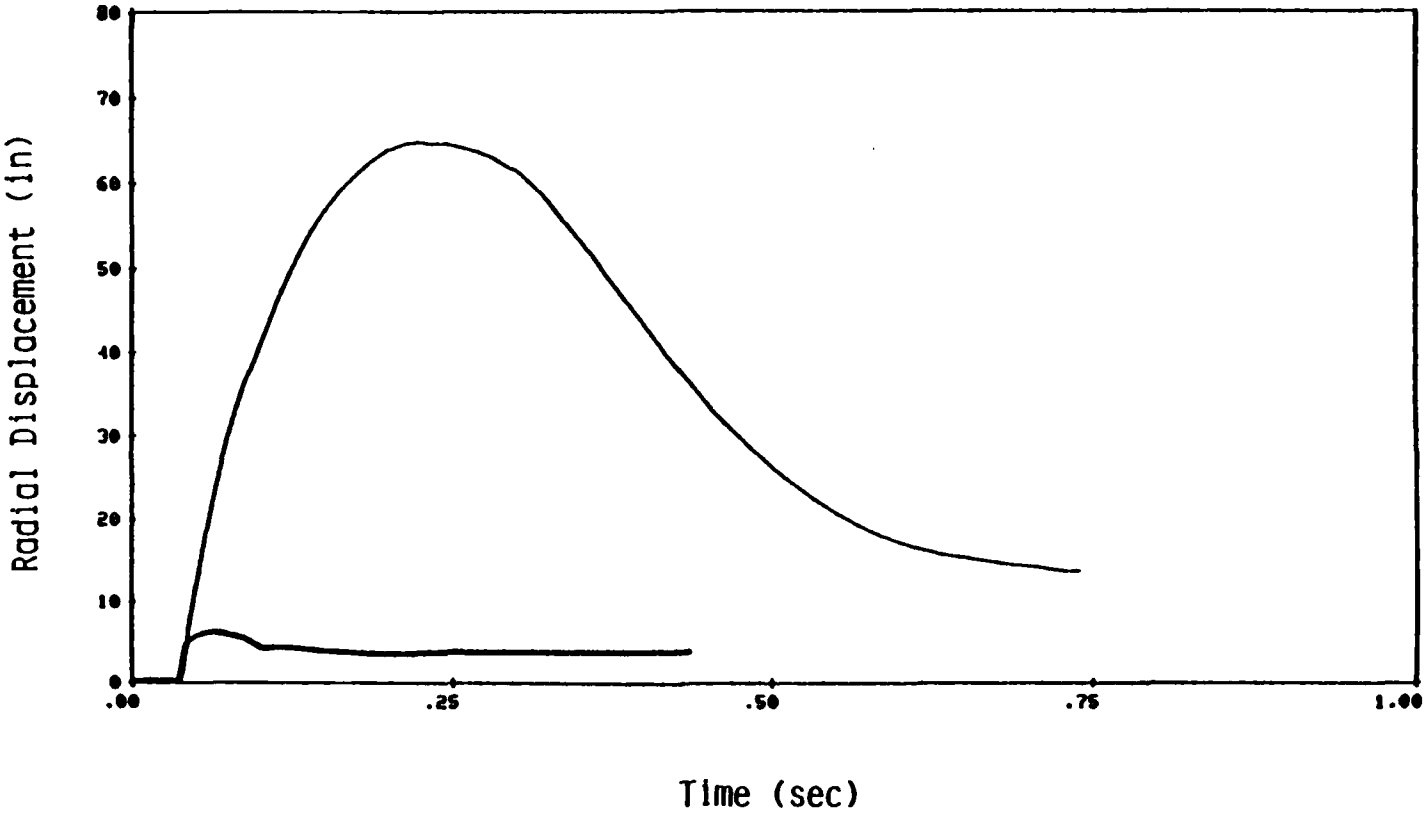


Figure 2.6. Comparison between PILEDRIVER displacement data (light curve) and the noneffective stress law calculation 204 meters from the source.

calculation in which the effective stress law was not used, i.e., the pore fluid pressure, $p_f$, in Equation (2.10) was assumed to be zero for all strain states and, therefore, the dry granite strength was not influenced by effective stress. The difference between these two calculations is quite significant, a factor of approximately 15 in peak displacement for instance, with the effective stress model providing good agreement with the data.

In addition, the final cavity radius calculated by the effective stress model was 40 meters, also a good agreement with PILEDRIVER cavity measurements. The cavity radius from the noneffective stress calculation was 26 meters. It is interesting that the difference between the effective stress and noneffective stress cavity radii is very close to the difference between NTS cavities in granite and those reported by the French from their granite test area in the Sahara.

The effective stress model was used by Day, Rimer and Cherry (1981) to perform a two-dimensional (axisymmetric) finite difference simulation of the PILEDRIVER event in order to determine the relation between spall and surface wave generation. Figure 2.7 shows a comparison between calculated ground motion and data recorded from the event. This data requires a two-dimensional simulation because of the influence of the free surface on the ground motion.

The results shown in Figures 2.3, 2.4 and 2.7 along with the comparison with cavity radius data suggest that an effective stress law is able to provide a satisfactory explanation of the PILEDRIVER ground motion data. Unfortunately, this type of data from underground nuclear tests is not frequently obtained. In fact, the PILEDRIVER data is unique in terms of the large amount of data available and the extent of both surface and subsurface coverage provided. Therefore, if further verifications of both the air-filled porosity and the effective stress constitutive models are

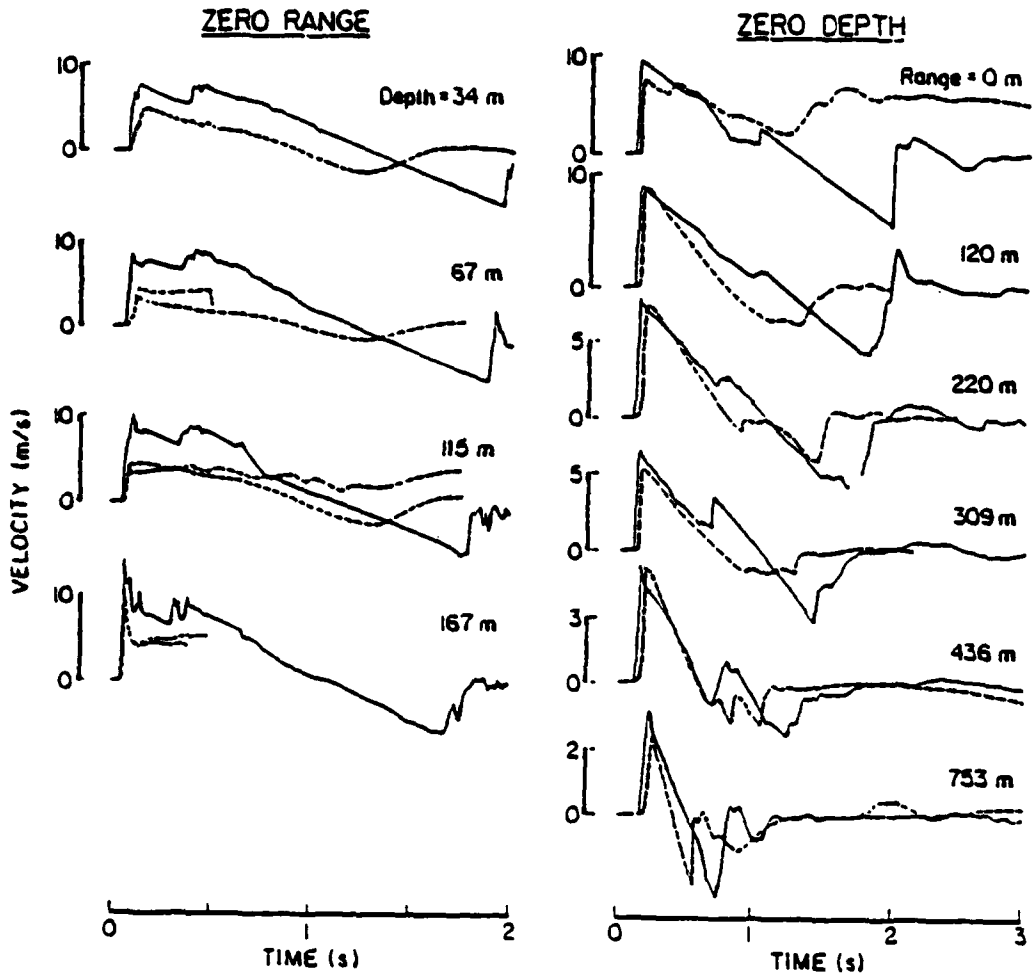


Figure 2.7. Vertical velocity time-histories (positive up) obtained from the two-dimensional simulation of Day, Rimer and Cherry (1981) compared with recorded velocities for PILEDRIVER.

to be obtained, it would seem logical that we use less expensive, small scale explosive tests. Data from such tests has recently become available. In the remainder of this report, we show the results of applying these models to this data.

# III. THE GROUT EXPERIMENTS

As part of the Defense Nuclear Agency (DNA) late-time containment program for underground nuclear testing, SRI International has, since 1976, been conducting small scale laboratory experiments to study explosion phenomenology related to the containment of the cavity gas. The initial experiments involved casting a 12 inch diameter sphere of either 2C4 or low density LD2C4 grout around a lucite-encased sphere of high explosive (3/8 gm of PETN), placing this grout sphere in a pressurized water tank to simulate overburden pressure, and detonating the PETN. While maintaining overburden pressure, the sphere was then hydrofractured from the explosively formed cavity using a tube emplaced preshot. Hydrofracture breakdown pressures from these tests are compared with breakdown pressures from precast (unexploded) spheres to obtain an estimate of the magnitude of the explosively formed residual stress fields. Figure 3.1 shows the experimental apparatus. A detailed description of these experiments and a discussion of the experimental results may be found in Cizek and Florence (1981).

Recently, SRI has begun to emplace particle velocity gauges inside the grout spheres (Cizek and Florence, 1981). These gauges consist of concentric circular current-carrying loops of wire cast symmetrically about the charge. A magnetic field is generated normal to the plane of the loops by passing current through a coil which surrounds the sphere. Charge detonation produces radial motion of the loops that cut the magnetic flux lines. In accordance with Faraday's law, the voltage induced in each conducting loop is proportional to the particle velocity. Records of radial particle velocity versus time obtained from these gauges have proved to be reproducible from shot to shot.

In addition to these experiments, DNA has supported the measurement of material properties for 2C4 and LD2C4 grout. These measurements have been made at SRI and Terra Tek, Inc. (Cooley, et al., 1982). They include static load-unload tests under uniaxial strain conditions, hydrostatic compression tests, triaxial

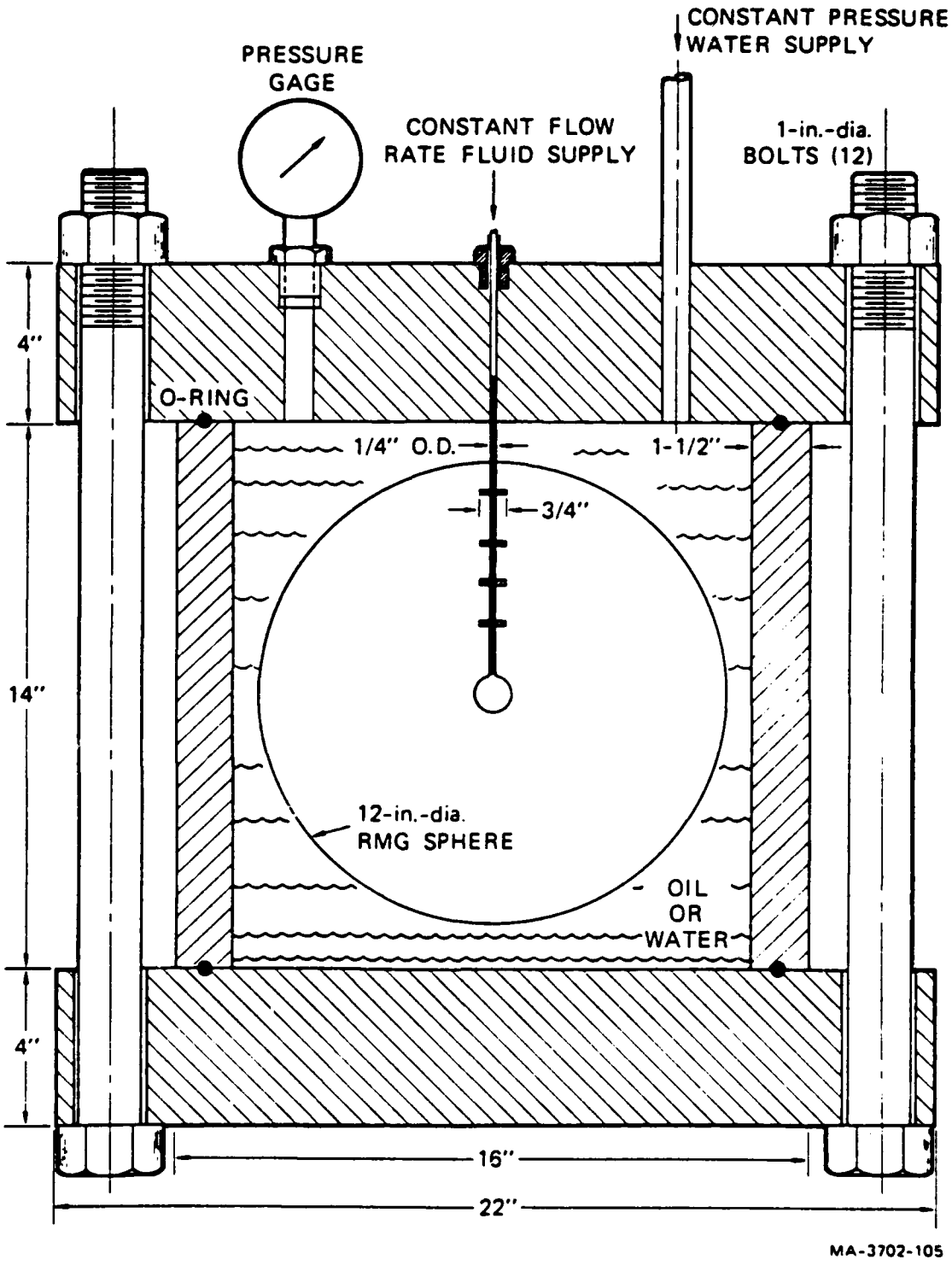


Figure 3.1. Grout spheres experiment apparatus (Cizek and Florence, 1981).

compression tests on both virgin samples and on samples damaged by hydrostatic compression to 4 Kbar and subsequent decompression, ultrasonic velocity tests and porosity, water content and density measurements.

Table 3.1 and Figures 3.2, 3.3, and 3.4 summarize the results of these tests. The data given in the table and in the figures were used in the effective stress simulation of the experiments. However, the strength data of Figure 3.4 were modified to account for the fact that the triaxial tests were not conducted either on dry samples or in an environment in which the pore fluid pressure was monitored during the test.

In the absence of strength tests on dry grout samples, we assumed that the dry failure surface was simply an upward extension of the sloped portion of the intact failure surface shown in Figure 3.4,

$$Y = a + b\bar{P} \ . \tag{3.1}$$

For 2C4 grout, we obtained the best agreement with the particle velocity data using

$$\begin{aligned} a &= 0.09 \text{ Kb} \\ b &= 1.6 \end{aligned} \tag{3.2}$$

while for LD2C4 grout, we used

$$\begin{aligned} a &= 0.055 \text{ Kb} \\ b &= 1.5 \ . \end{aligned} \tag{3.3}$$

Both the slopes and the intercepts given by Equations (3.2) and (3.3) are within the constraints imposed by the data shown in Figure 3.4. The grout strength is now modified by pore fluid pressure according to

$$Y = a + b(\bar{P} - p_f) \tag{3.4}$$

where $p_f$ is calculated using Equation (2.9).

TABLE 3.1

MATERIAL PROPERTIES FOR 2C4 ROCK MATCHING GROUT
AND LD2C4 LOW DENSITY GROUT

| Property | 2C4 | LD2C4 |
|---|---|---|
| Density (gm/cc) | 2.205 | 1.921 |
| P-Wave Velocity (m/s) | 3318.0 | 3128.0 |
| S-Wave Velocity (m/s) | 1792.0 | 1629.0 |
| Air-Filled Porosity (%) | 1.5 | 13.4 |
| Unconfined Strength (bar) | 270 ± 30 | 220 ± 30 |
| Tensile Strength (bar) | 36 ± 10 | 31 ± 10 |

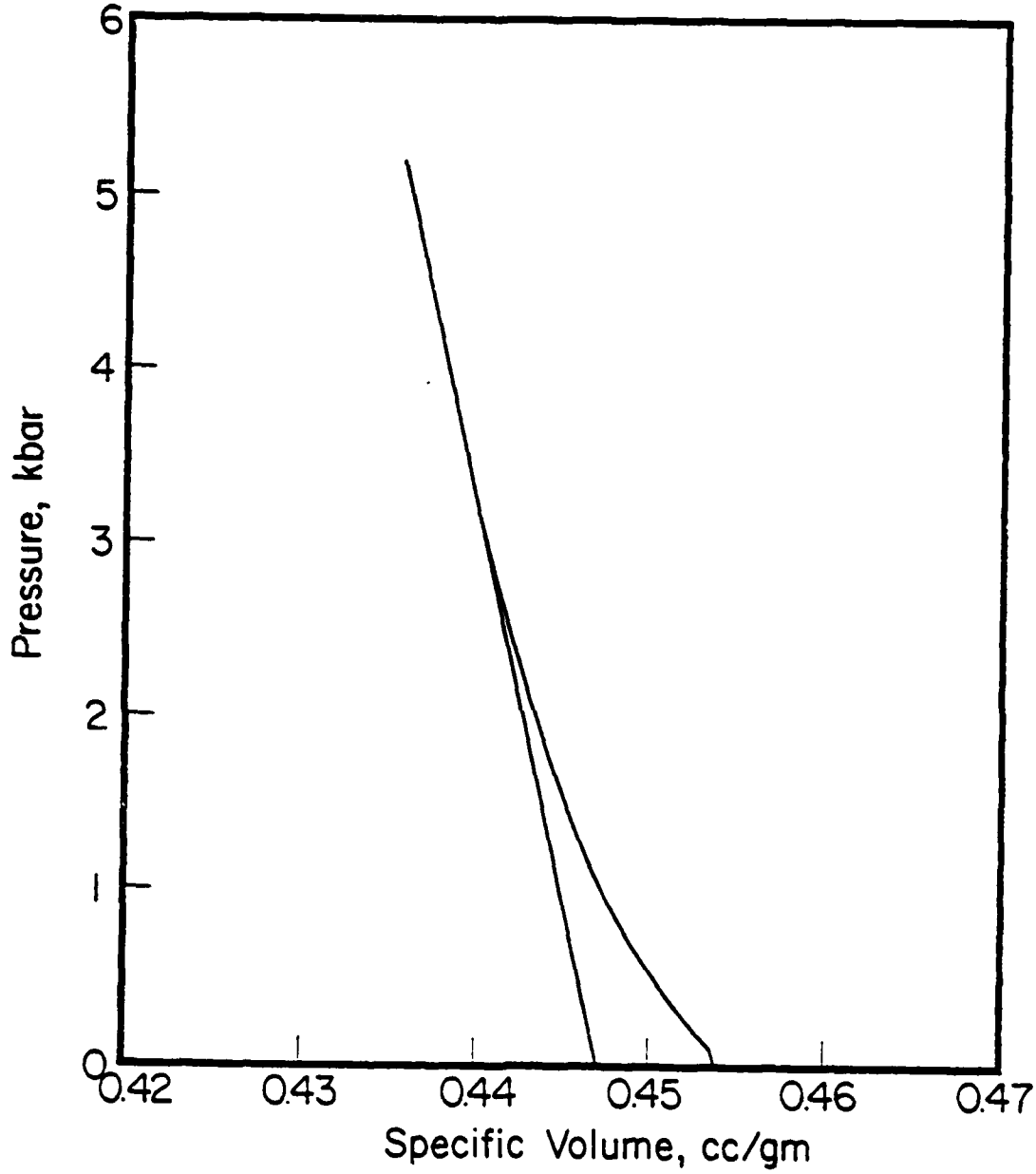


Figure 3.2. Crush curve for 2C4 grout.

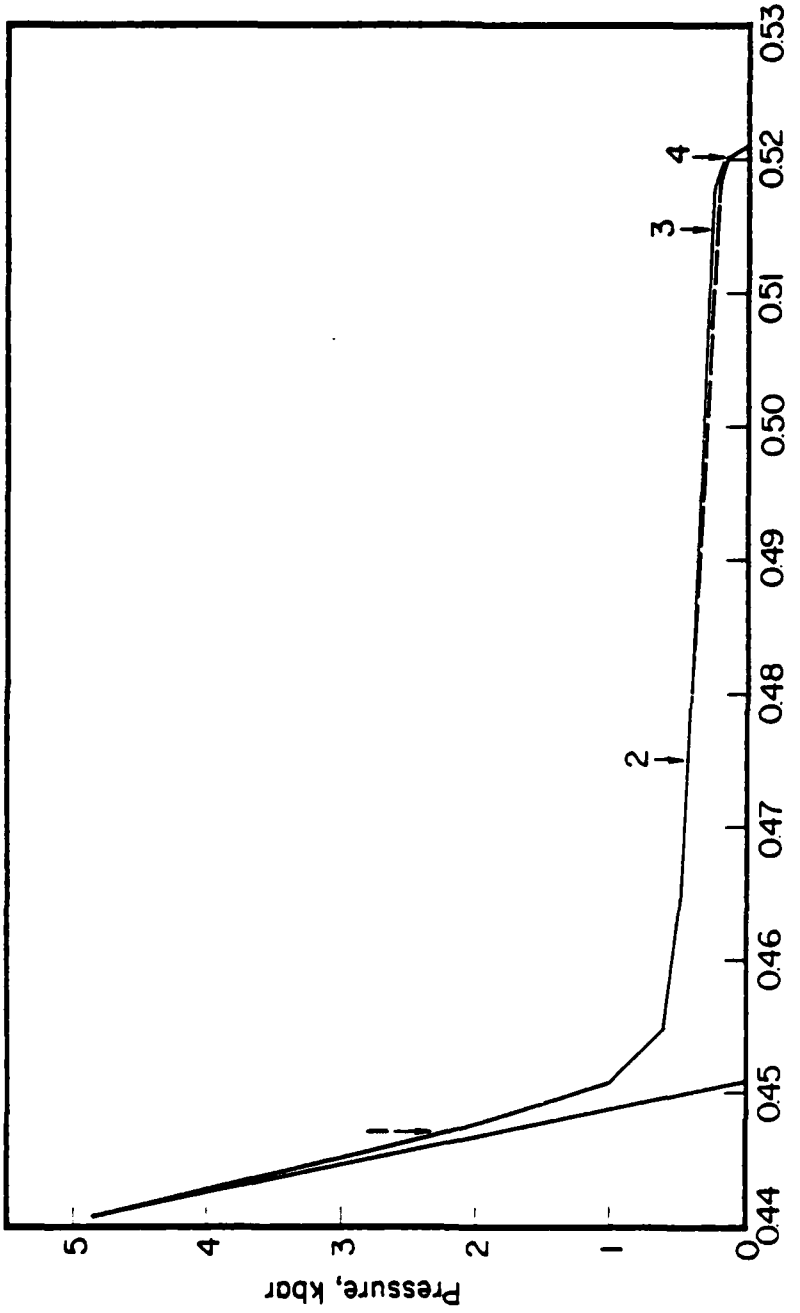


Figure 3.3. Crush curve for LD2C4 grout. The solid curve was used for the RDD model calculation and the dotted curve for the effective stress calculation. The arrows indicate the approximate loadings corresponding to the velocity peaks at the four gauges.

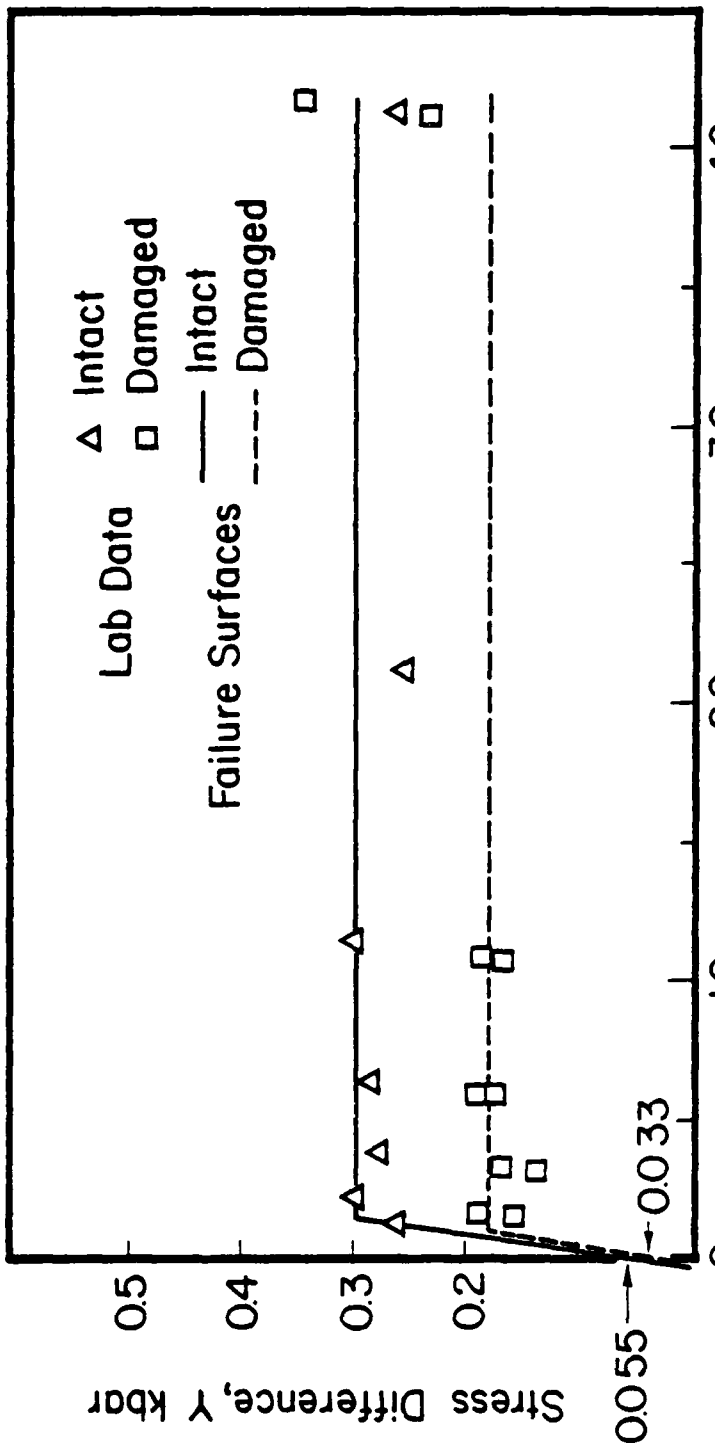


Figure 3.4. Failure surface for 2C4 rock matching grout.

# IV. SIMULATION OF EXPERIMENTS IN 2C4 AND LD2C4 GROUT

In this section, we present three simulations of high explosive experiments in grout and compare the results of these simulations with particle velocity measurements at distances of 1.27 cm, 1.9 cm, 2.54 cm and 4.0 cm from the charge center.

The first simulation used the material properties for 2C4 grout but no effective stress law, and the strength used in the simulation was that denoted in Figure 3.4 as the "intact failure surface." Figures 4.1, 4.2, 4.3, and 4.4 compare the particle velocities calculated from the simulation with those measured during the experiment. At all ranges, the calculated velocity pulse is too wide during the positive phase and too narrow during the negative phase.

The second simulation used the material properties for 2C4 grout and included the modification of material strength due to pore fluid pressure (effective stress) given by Equation (3.4). The comparison between calculated particle velocities and those measured are shown in Figures 4.5, 4.6, 4.7 and 4.8. At all ranges, we obtain excellent agreement with measured data from effective stress law simulation.

The consequences of these two simulations (with and without effective stress) on seismic coupling is interesting and is shown by the RVP spectra in Figure 4.9. The RVP spectrum with effective stress is peaked, with the spectral peak about a factor of two larger than the spectral amplitude at low frequencies. The RVP spectrum without effective stress is flat and greater than the effective stress spectrum at low frequencies by a factor of 1.5.

Peaking of the RVP spectrum is a direct consequence of the width and amplitude of the negative portion of the velocity pulse, and the frequency at which the peak occurs is approximately equal to the period of the pulse. The effective stress model produces the correct shape for the velocity pulse during both the positive and negative phases of the pulse by providing high material strength

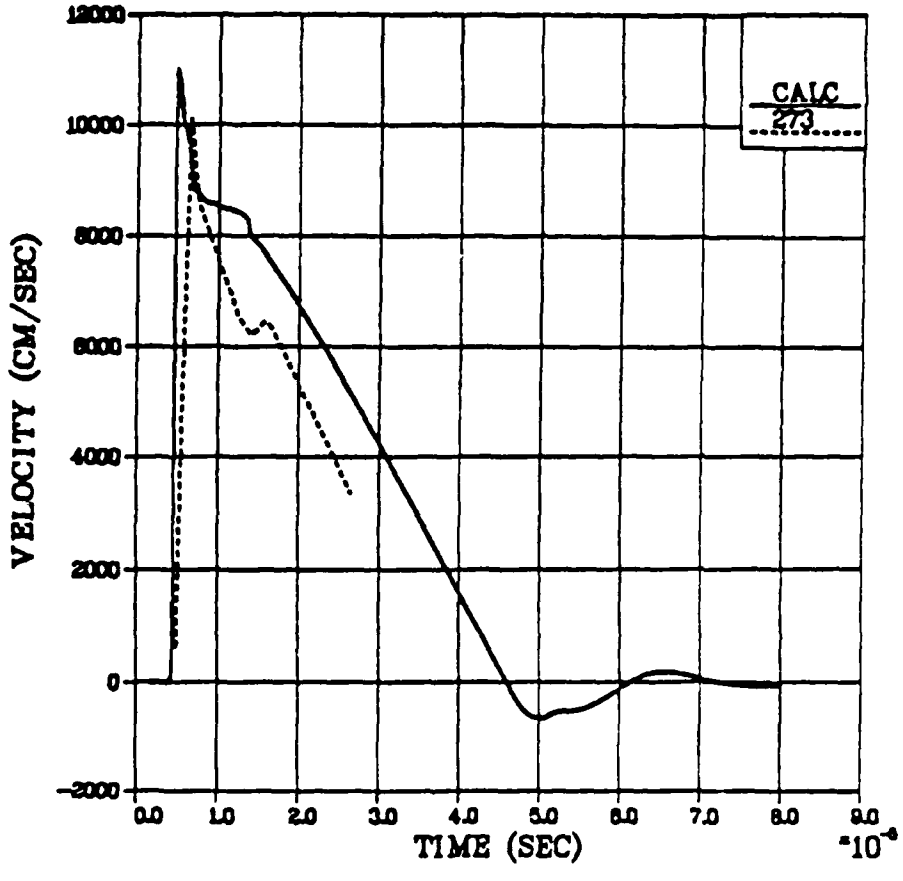


Figure 4.1. Comparison between measured velocities in 2C4 grout and those calculated from a noneffective stress law simulation at 1.27 cm. In this and all subsequent comparisons the solid curves are calculated, and dashed curves are measured velocities.

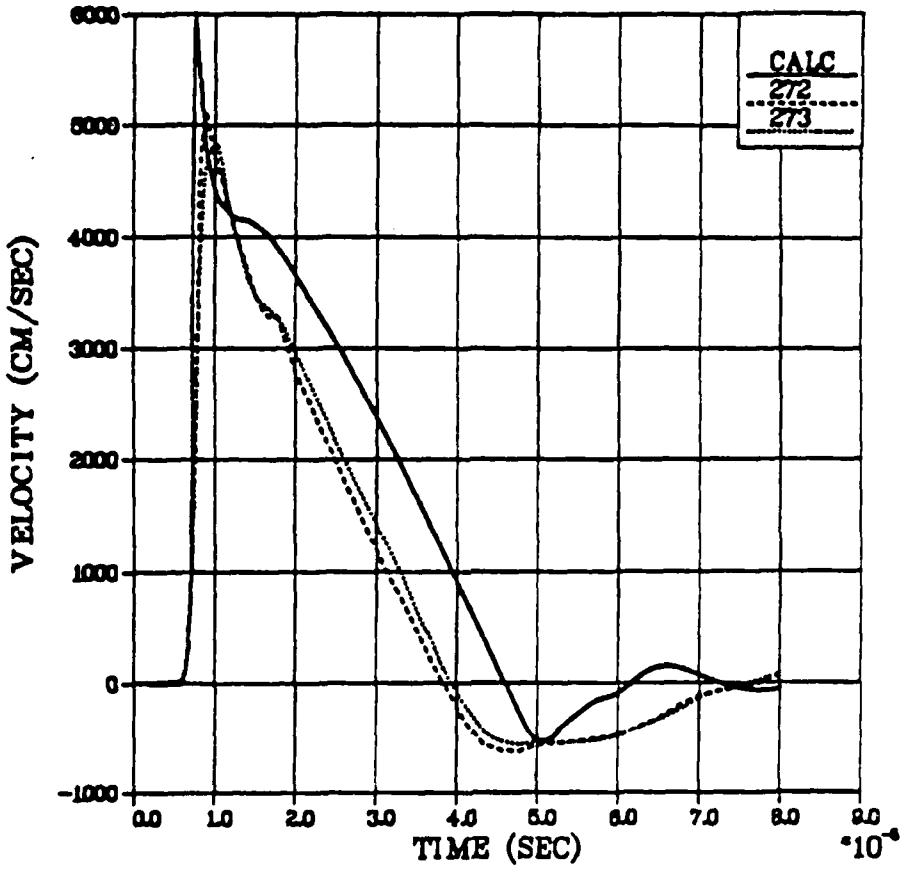


Figure 4.2. Comparison between measured velocities in 2C4 grout and noneffective stress law simulation at 1.9 cm.

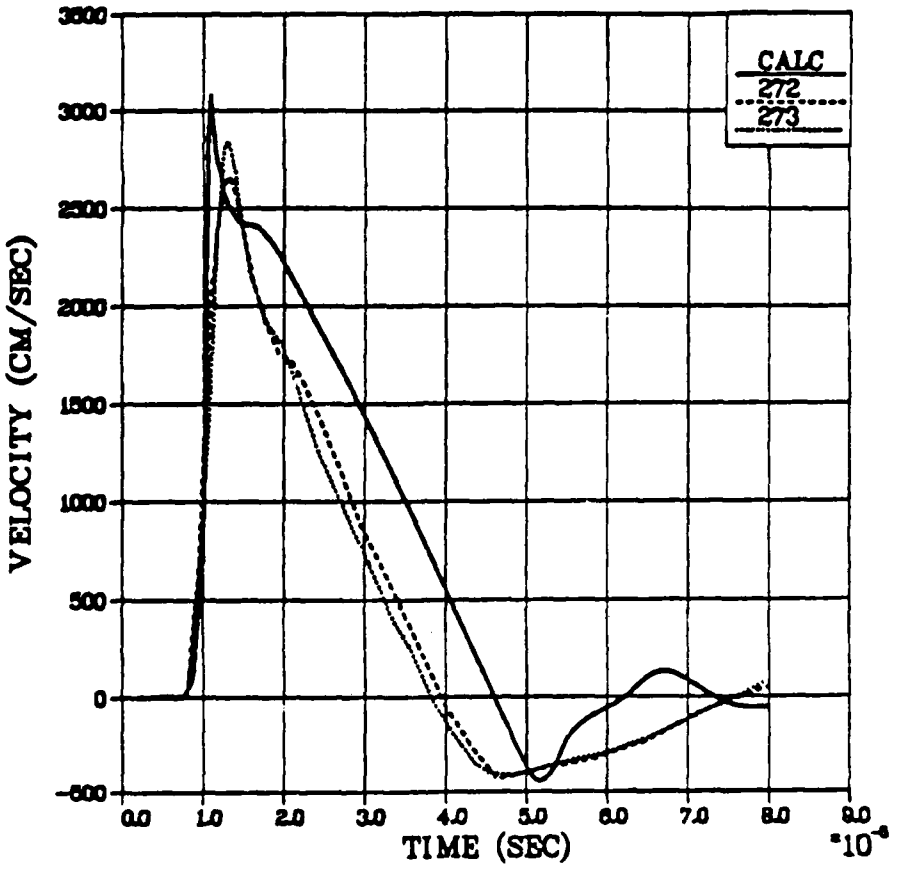


Figure 4.3. Comparison between measured velocities in 2C4 grout and noneffective stress law simulation at 2.54 cm.

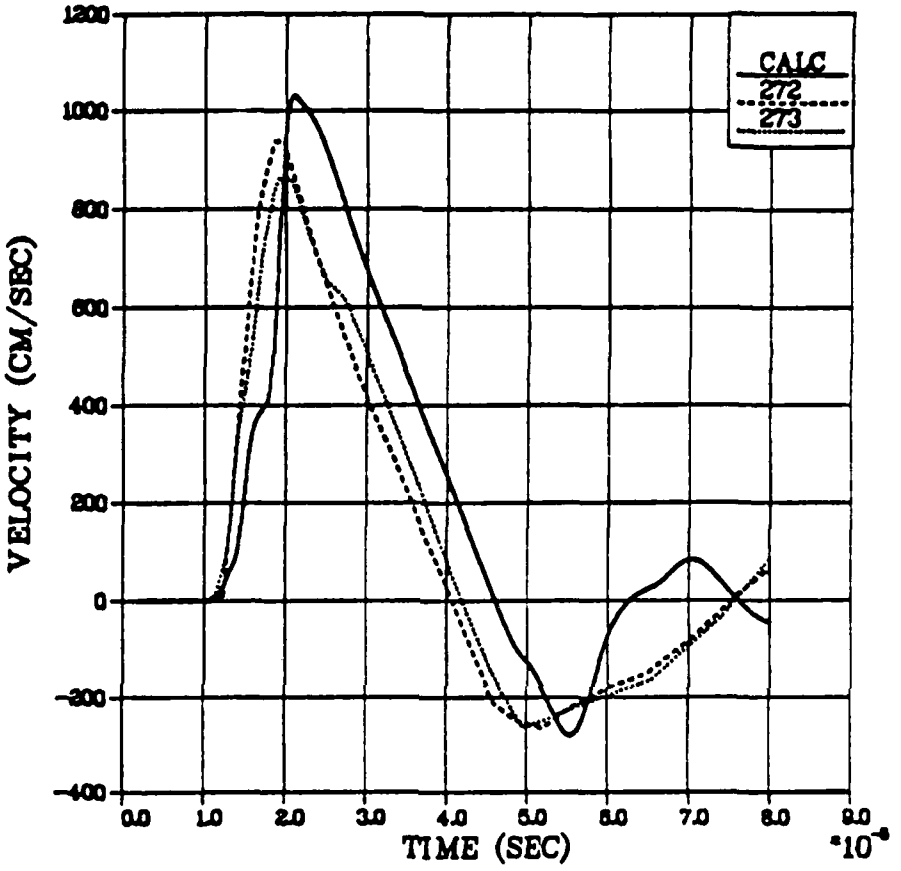


Figure 4.4. Comparison between measured velocities in 2C4 grout and noneffective stress law simulation at 4.0 cm.

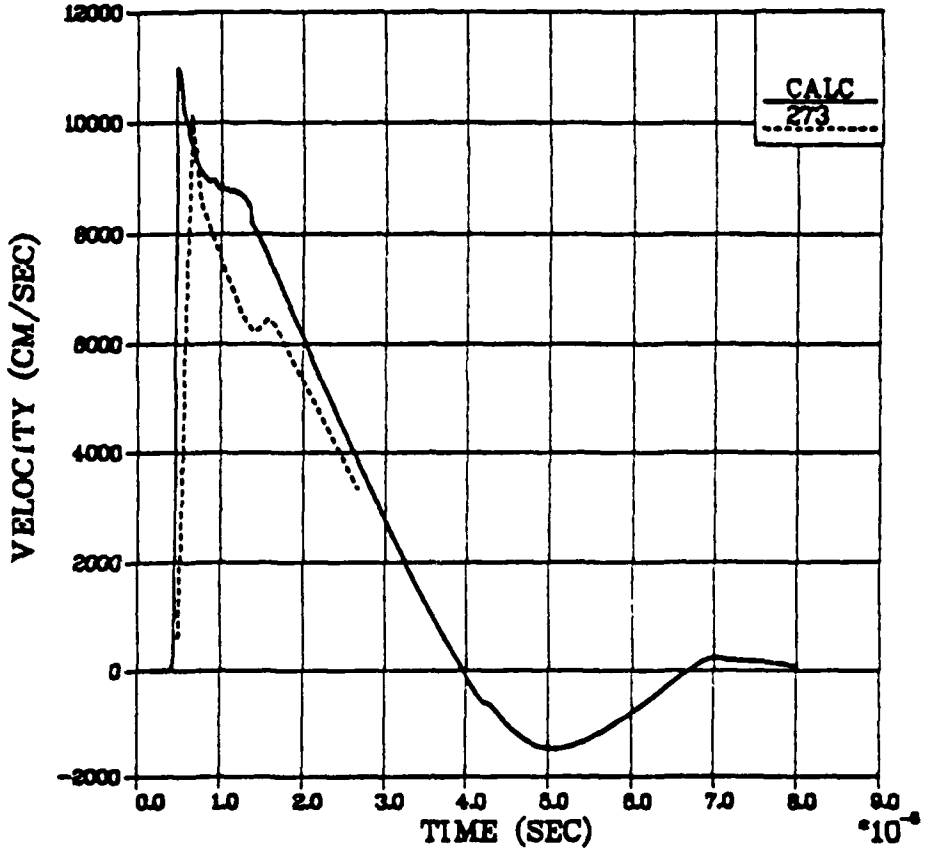


Figure 4.5. Comparisons between measured velocities in 2C4 grout and effective stress law simulation at 1.27 cm.

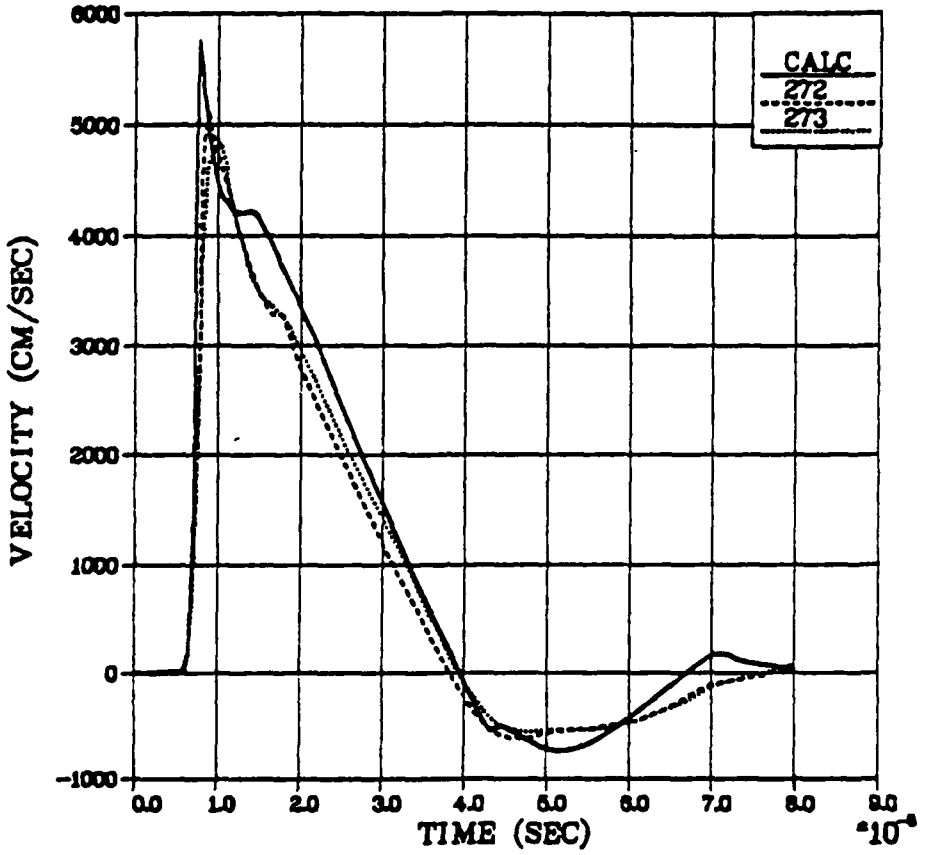


Figure 4.6. Comparisons between measured velocities in 2C4 grout and effective stress law simulation at 1.9 cm.

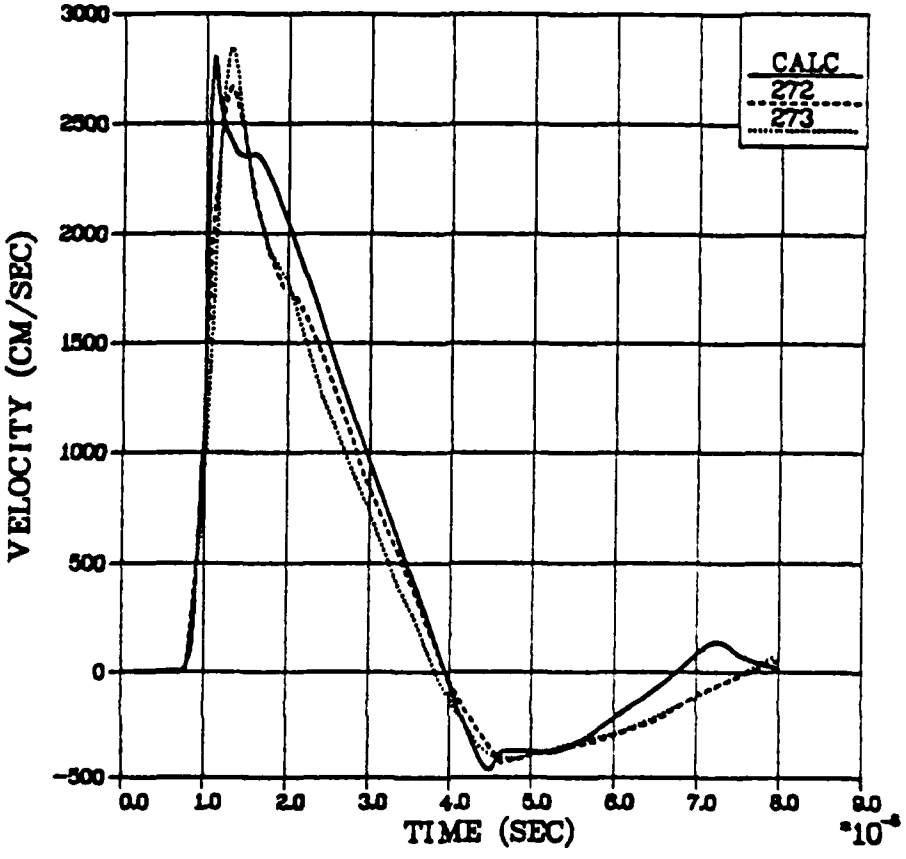


Figure 4.7. Comparisons between measured velocities in 2C4 grout and effective stress law simulation at 2.54 cm.

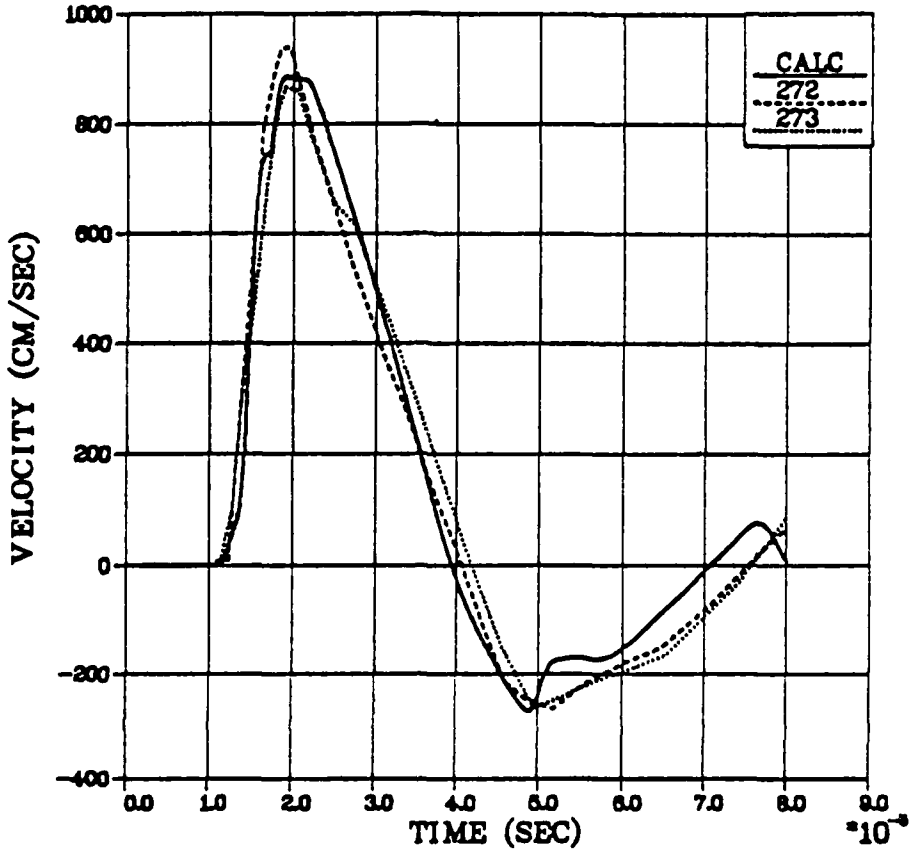


Figure 4.8. Comparisons between measured velocities in 2C4 grout and effective stress law simulation at 4.0 cm.

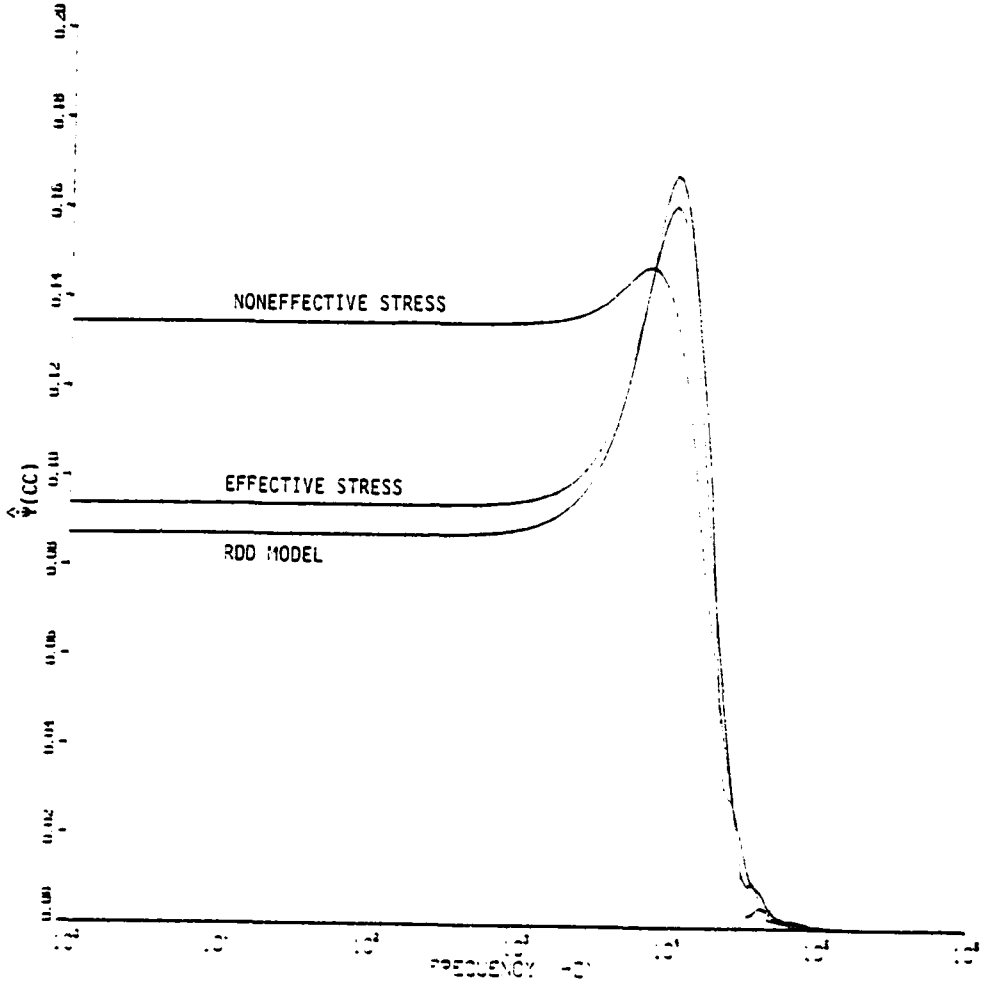


Figure 4.9. Spectra of the reduced velocity potentials from the noneffective stress and the effective stress simulations. Also included is the spectra from the RDD model (Rimer and Lee (1982)).

during the initial stages of pore collapse and then lowering the strength during the final stages. The high strength retards the velocities during the positive phase while the low strength broadens the negative portion of the pulse.

The third simulation used the material properties for LD2C4 grout and included the effective stress constitutive model. The comparison between the calculated particle velocities and those measured during the grout experiments are shown in Figures 4.10, 4.11, 4.12, and 4.13. The agreement between the calculated results and the data is acceptable, indicating that the effective stress model is applicable to a wide range of air void porosities.

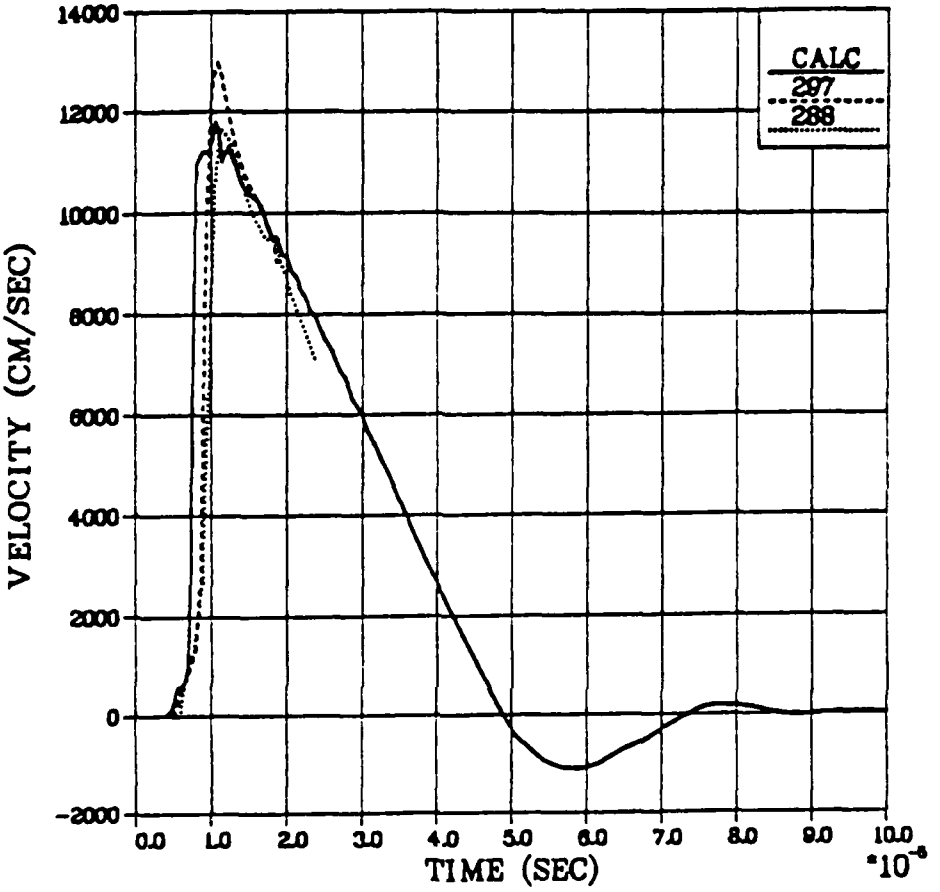


Figure 4.10. Comparisons between measured velocities in LD2C4 grout and effective stress law calculation at 1.27 cm.

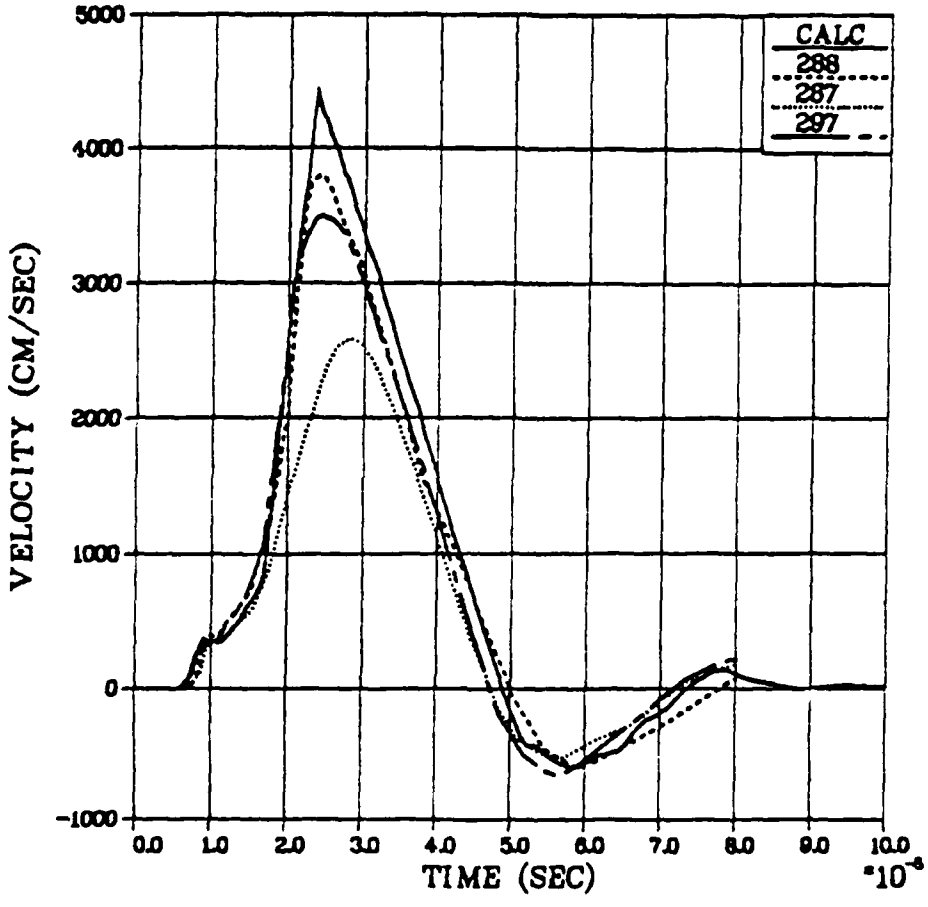


Figure 4.11. Comparisons between measured velocities in LD2C4 grout and effective stress law calculation at 1.90 cm.

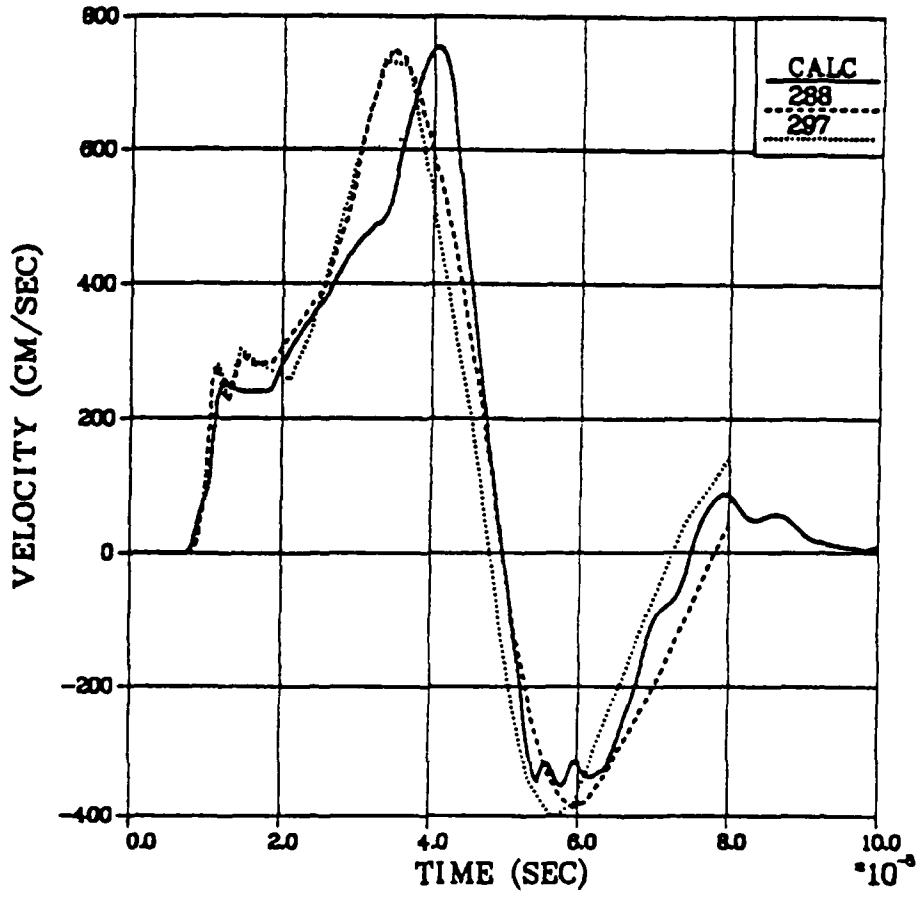


Figure 4.12. Comparisons between measured velocities in LD2C4 grout and effective stress law calculation at 2.54 cm.

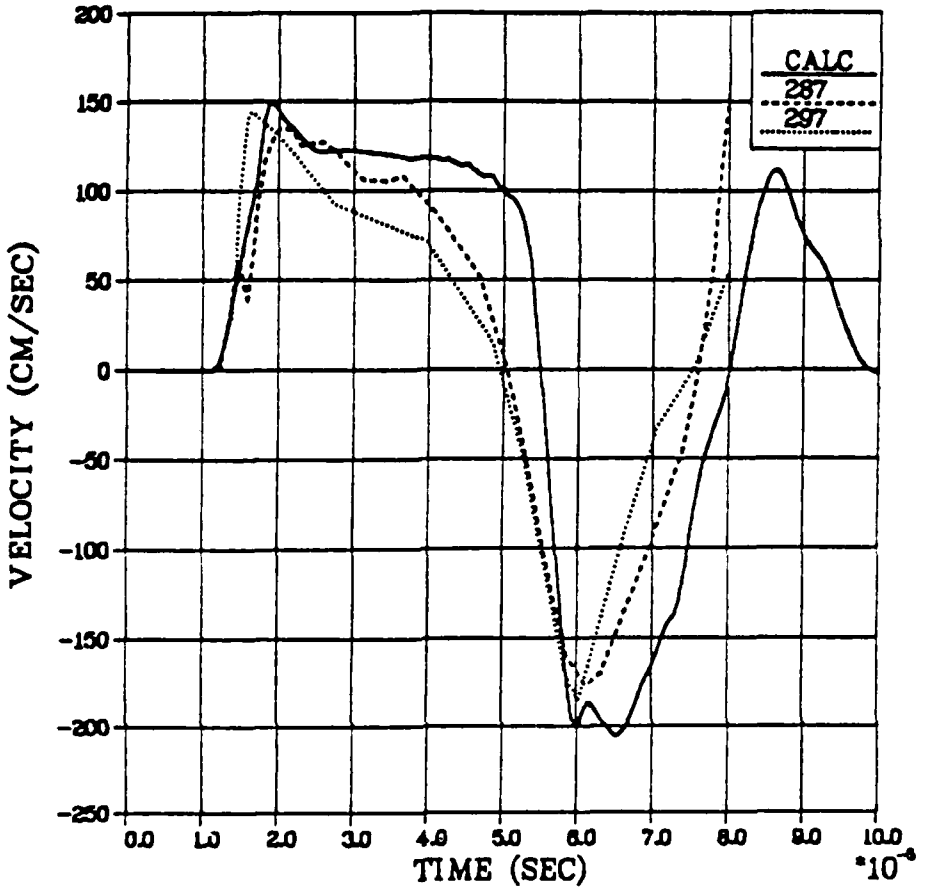


Figure 4.13. Comparisons between measured velocities in LD2C4 grout and effective stress law calculation at 4.0 cm.

# V. UNIQUENESS

Other constitutive models can be constructed which provide as good (or better) a fit to the data as the effective stress law results shown in Section IV. Rimer and Lie (1982) have developed such a model. They discuss in detail a complicated rate dependent and damage dependent set of constitutive models (referred to as the RDD model) which they used to simulate the SRI experiments in 2C4 and LD2C4 grout. The RDD model has three important features: a failure surface which is strain rate dependent upon loading; a rate dependent stress relaxation from this failure surface to a damaged failure surface upon unloading; and a reduced shear modulus upon loading. Both the rate of deviatoric stress relaxation and the failure strength of the damaged grout are made functions of the amount of damage, as is the shear modulus. The deviatoric stress relaxation to the damaged failure surface is accomplished using a Maxwell solid approach.

This model successfully matches the SRI data in 2C4 and LD2C4 grout (Figures 5.1, 5.2, 5.3, 5.4, 5.5, 5.6, 5.7, and 5.8), and the seismic coupling is approximately the same as that from the effective stress law (Figure 4.9). However, the complicated RDD model requires many assumptions regarding material properties which are certainly not easily verified (and indeed may be impossible to verify) from laboratory material properties tests.

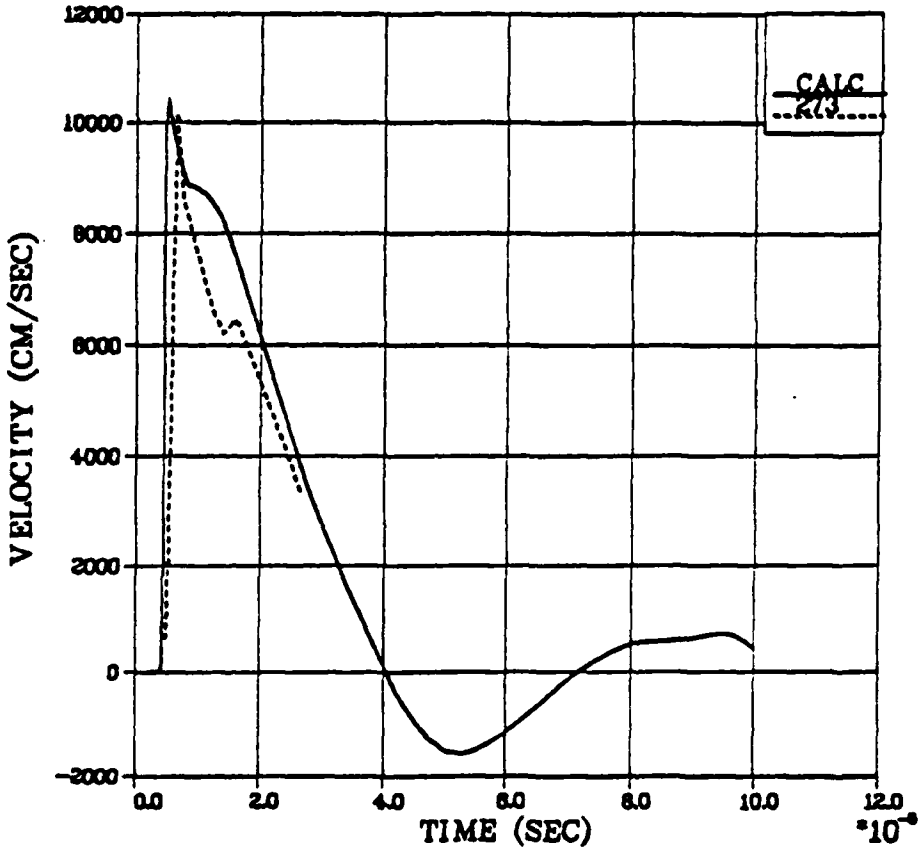


Figure 5.1. Comparison between measured particle velocities from SRI 2C4 grout test 273 and results of RDD model calculation at a radial range of 1.27 cm.

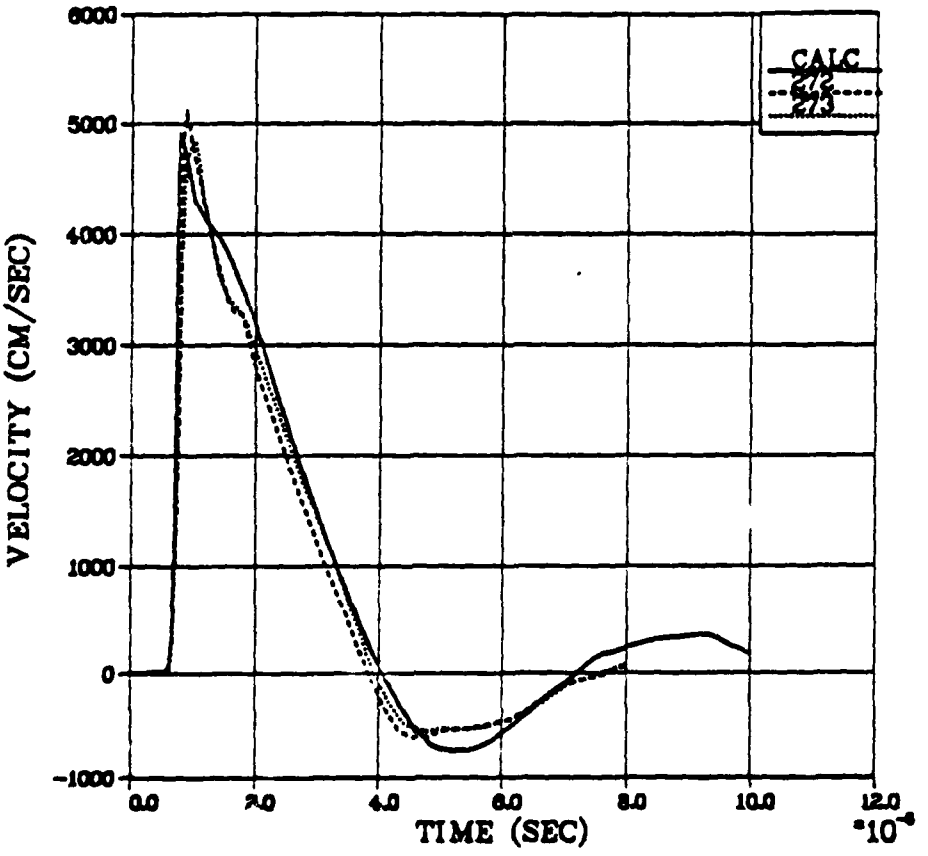


Figure 5.2. Comparisons between measured velocities from 2C4 grout tests 272 and 273 and results of RDD model calculation at 1.9 cm.

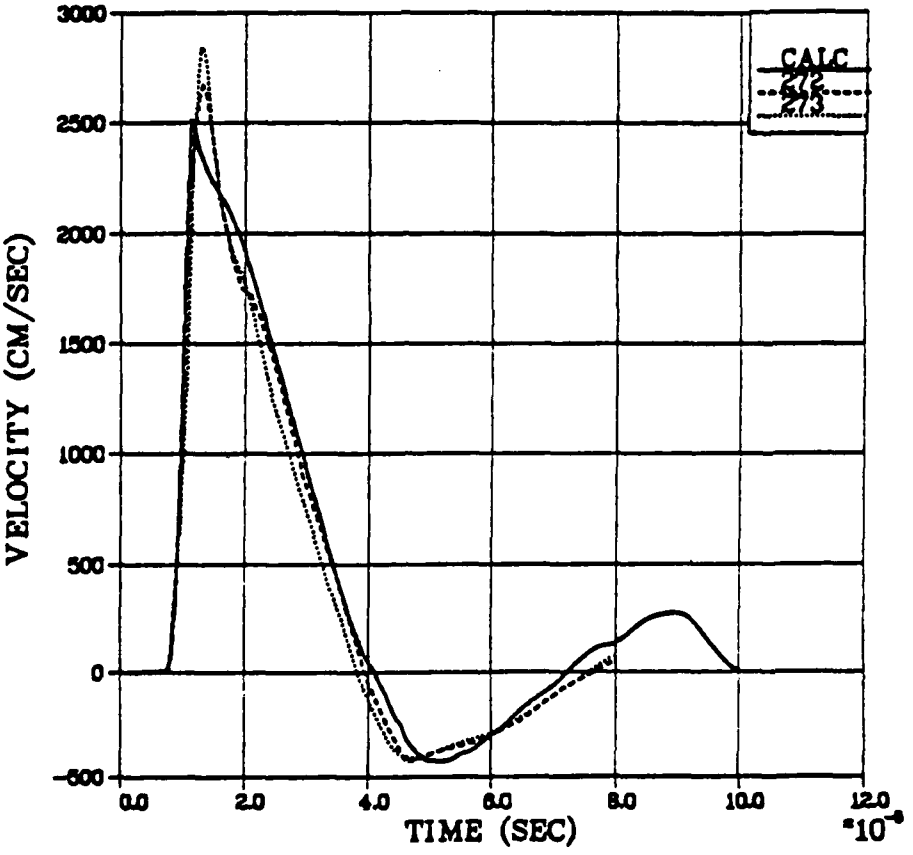


Figure 5.3. Comparisons between measured velocities in 2C4 grout and RDD model simulation at 2.54 cm.

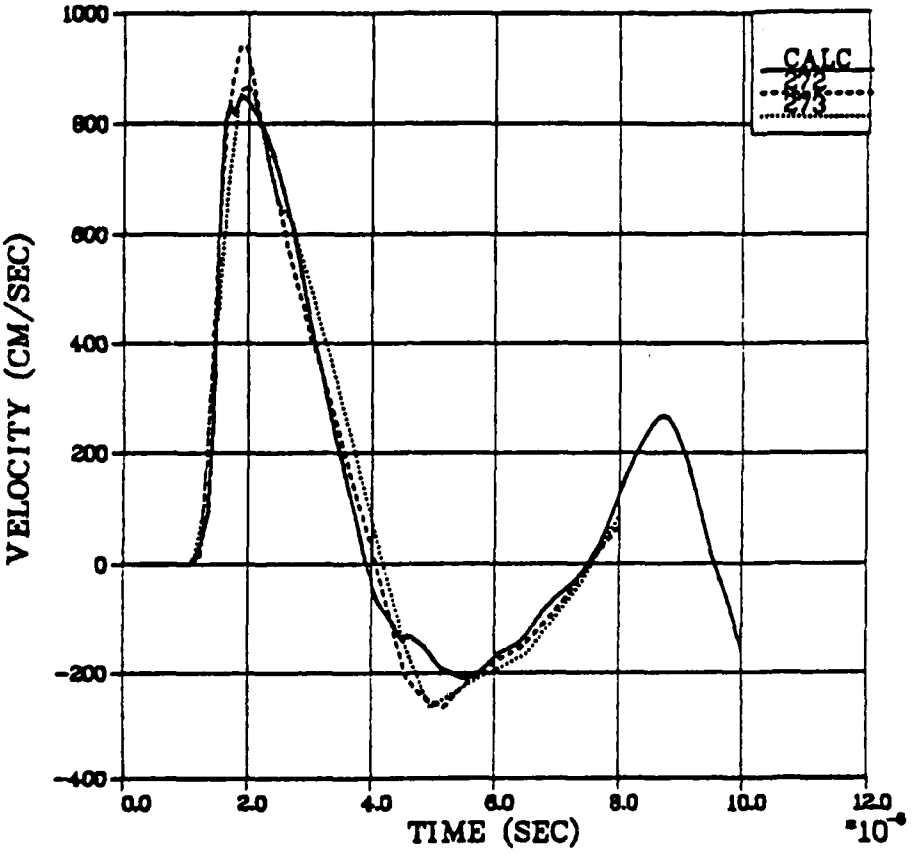


Figure 5.4. Comparisons between measured velocities in 2C4 grout and RDD model simulation at 4.0 cm.

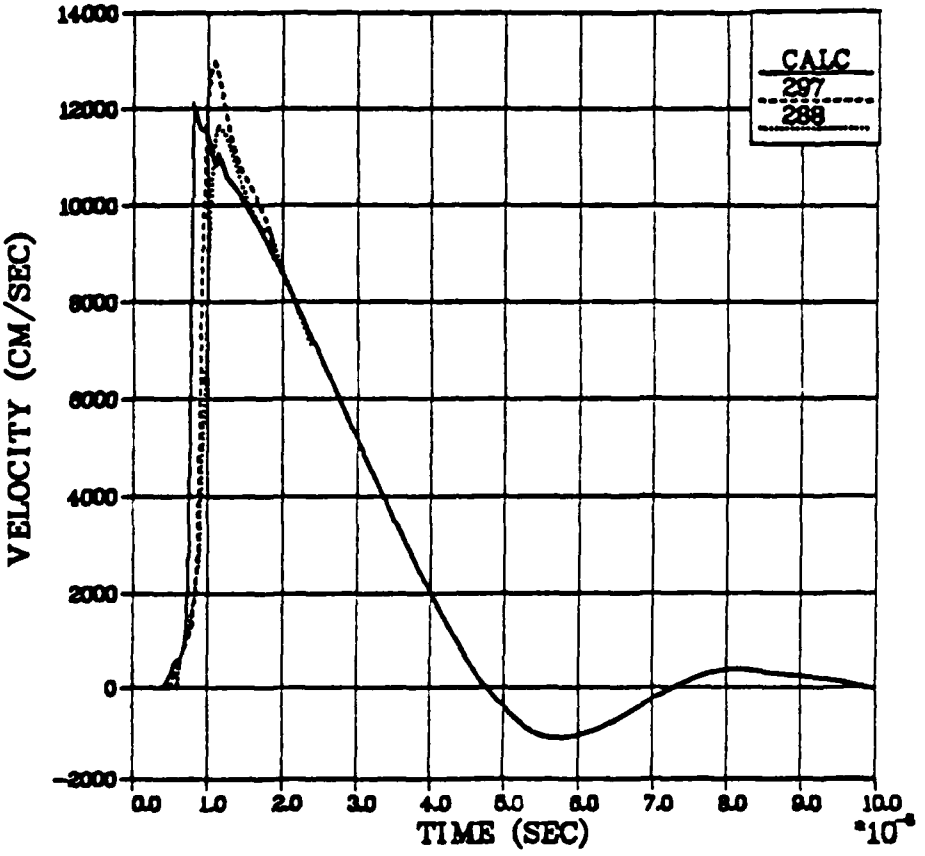


Figure 5.5. Comparisons between measured particle velocities from SRI LD2C4 grout tests 288 and 297 and results of RDD model calculation at a radial range of 1.27 cm.

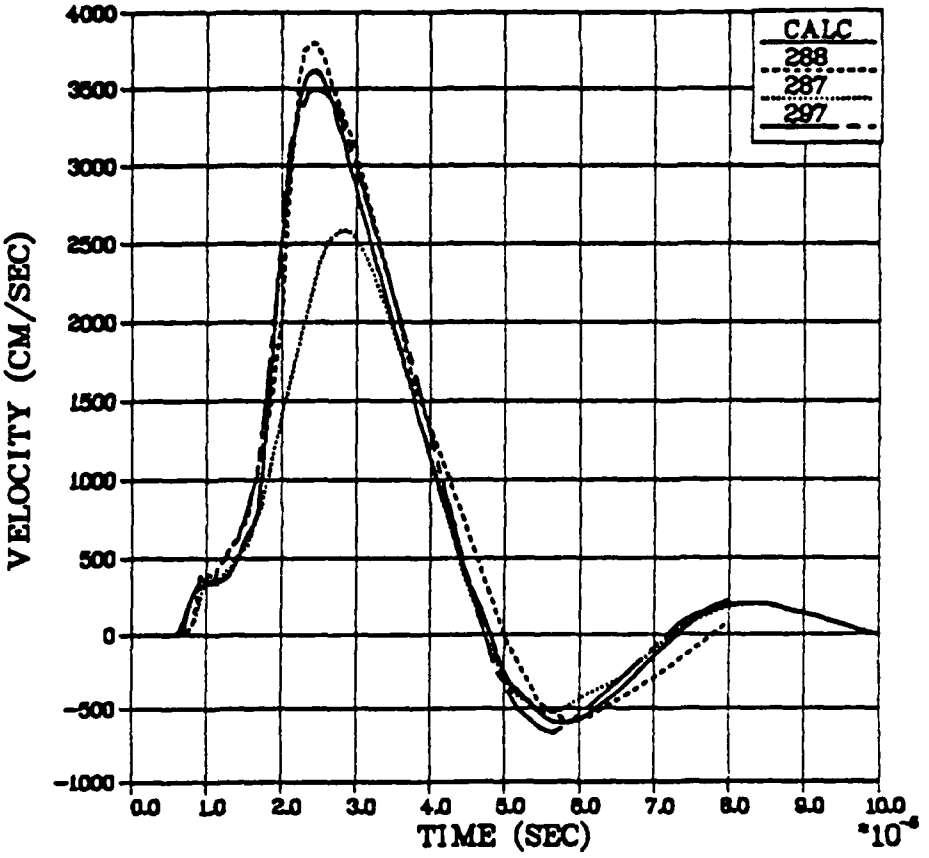


Figure 5.6. Comparisons between measured velocities in LD2C4 grout and RDD model simulation at 1.9 cm.

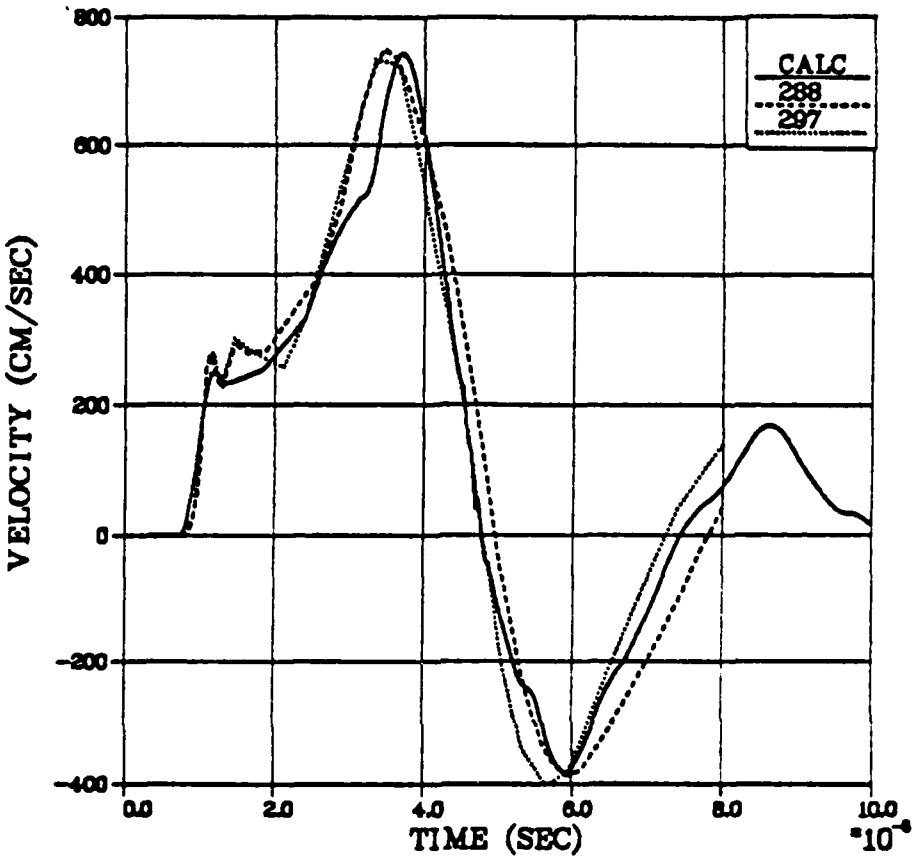


Figure 5.7. Comparisons between measured velocities in LD2C4 grout and RDD model calculation at 2.54 cm.

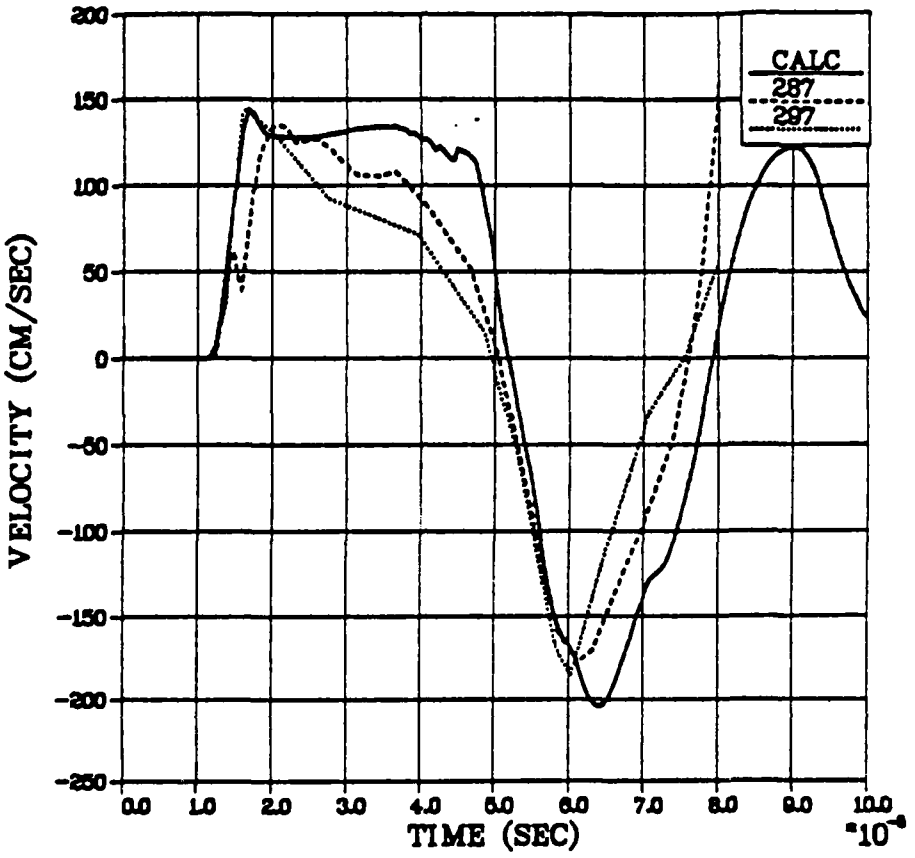


Figure 5.8. Comparisons between measured velocities in LD2C4 grout and RDD model calculation at 4.0 cm.

# VI. CONCLUSIONS AND RECOMMENDATIONS

We have reviewed the current status of two specific constitutive models which severely affect seismic coupling. These models were the irreversible collapse of air-filled porosity and the modification of material strength due to pore fluid pressure, i.e., effective stress.

We have shown how these models provide a very simple, straightforward explanation of ground motion data over a wide range of yields (61 KT, nuclear to 3/8 gram, PETN) and air void porosities (0.1 percent to 13.4 percent). The most critical material properties required by these models for near field ground motion and seismic coupling predictions are the dry strength, the pressure at which all air void porosity is removed, and the initial air void porosity.

These results have served to reenforce our confidence in the ability of these models to predict near field ground motion and seismic coupling effects. We recommend intensive continuation of their application, not only to explosion sites which have preshot measurements of material properties and/or near field ground motion measurements, but also to sites where explosion yield can only be estimated from far field seismic measurements.

## VII. ACKNOWLEDGMENT

The authors wish to acknowledge the contribution to this work of Dr. Carl E. Keller, Chief, Containment Division, DNA Field Command. He not only made the grout data available to us but had the foresight and tenacity to insist on its acquisition.

# VIII. REFERENCES


Bache, T. C., T. G. Barker, T. R. Blake, J. T. Cherry, D. G. Lambert, N. Rimer, and J. M. Savino (1975), "An Explanation of the Relative Amplitudes of the Teleseismic Body Waves Generated by Explosions in Different Test Areas at NTS," Systems, Science and Software Final Report submitted to Defense Nuclear Agency, DNA 3958F.

Brace, W. F. (1965), "Some New Measurements on the Linear Compressibility of Rock," JGR, 70, pp. 391-398.

Byerlee, J. D., (1979), "Experimental Study of Rock Friction with Application to Earthquake Prediction," Pure Appl. Geophys., p. 117.

Cherry, J. T. and F. L. Peterson (1970), "Numerical Simulation of Stress Wave Propagation from Underground Nuclear Explosions," in Engineering with Nuclear Explosives, Vol. 1, Available from the Clearing House for Federal Scientific and Technical Information, National Bureau of Standards, Springfield, Virginia.

Cherry, J. T., C. B. Archambeau, G. A. Frazier, A. J. Good, K. G. Hamilton, and D. J. Harkerider (1973), "The Teleseismic Radiation Field from Explosions: Dependence of the Seismic Amplitudes Upon Properties of Materials in the Source Region," Systems, Science and Software Final Report submitted to Defense Nuclear Agency, DNA 3113Z.

Cherry, J. T., N. Rimer, W. O. Wray (1975), "Seismic Coupling from a Nuclear Explosion: The Dependence of the Reduced Displacment Potential on the Nonlinear Behavior of the Near Source Rock Environment," Systems, Science and Software Technical Report submitted to VELA Seismological Center, SSS-R-76-2742, September.

Cizek, J. C. and A. L. Florence (1981), "Laboratory Investigation of Containment in Underground Nuclear Tests," SRI International Final Report for 1980 submitted to Defense Nuclear Agency, DNA 5731F, February.

Cooly, C. H., R. H. Smith and J. F. Schatz (1982), "Properties of Tuffs, Grouts and other Materials," Terra Tek Final Report submitted to Defense Nuclear Agency, TR-82-05, January.

Day, S. M., N. Rimer, and J. T. Cherry (1981), "Surface Waves from Underground Explosions with Spall: Analysis of Elastic and Nonlinear Source Models," Systems, Science and Software Topical Report submitted to VELA Seismological Center, VSC-TR-82-11.

Dieterich, J. H. (1978), "Time Dependent Friction and the Mechanics of Stick-Slip," Pure Appl. Geophys., 116, pp. 790-806.

Garg, S. K. and A. Nur (1973), "Effective Stress Law for Fluid-Saturated Porous Rocks," JGR, 78, pp. 5911-5921.

Heard, H. C. (1970), "The Influence of Environment of the Inelastic Behavior of Rocks," in Engineering with Nuclear Explosives, Vol. 1, Available from the Clearing House for Federal Scientific and Technical Information, National Bureau of Standards, Springfield, Virginia.

Rimer N. and K. Lie (1979), "Spherically Symmetric Calculations of the SRI Grout Spheres Experiments for Four Different Laboratory Configurations," Systems, Science and Software Topical Report, SSS-R-80-4240, November.

Rimer, N. and K. Lie (1982), "Simulation of the Velocity Records from the SRI Grout Spheres Experiments," Systems, Science and Software Topical Report, SSS-R-82-5580.

Riney, T. D., G. A. Frazier, S. K. Garg, A. J. Good, R. G. Herrmann, L. W. Morland, J. W. Pritchett, M. H. Rice, and J. Sweet (1973), "Constitutive Models and Computer Techniques for Ground Motion Predictions," Systems, Science and Software Report submitted to Defense Nuclear Agency, DNA 3180F.

Scholz, C. H. and J. T. Engelder (1976), "The Role of Asperity Indentation and Ploughing in Rock Friction, I.," Int. J. Rock Mech. Min. Sci., 13, pp. 149-154.

Stephens, D. R. and E. M. Lilley (1970), "Loading-Unloading Pressure-Volume Curves for Rocks," in Engineering with Nuclear Explosives, Vol. 1.